Elsevier Editorial System(tm) for Progress in Oceanography
Manuscript Draft

Manuscript Number: PROOCE-D-11-00015R1

Title: Sub-surface small scale eddy dynamics from multi-sensor observations and modelling

Article Type: Full Length Article

Keywords: mesoscale eddy, multi-sensor, coastal altimetry, glider, regional modelling

Corresponding Author: Dr. Jerome bouffard, Ph.D.

Corresponding Author's Institution: IMEDEA (UIB-CSIC)

First Author: Jerome bouffard, Ph.D.

Order of Authors: Jerome bouffard, Ph.D.; Lionel Renault, PhD; Simon Ruiz, PhD; Ananda Pascual, PhD; Claire Dufau, PhD; Joaquin Tintoré, PhD

Abstract: The study of mesoscale and submesoscale [hereafter (sub)mesoscale] hydrodynamic features are essential for understanding heat and biogeochemical exchanges between the coastal and open ocean. In this context, a glider mission was carried out in August 2008, well co-localized and almost simultaneously with a JASON 2 altimetric pass in order to fully characterize currents associated with regional (sub)meso-scale processes regularly observed to the north of Mallorca (Mediterranean Sea). A synoptic view from satellite remote-sensing fields, before and during the glider mission, provided a descriptive picture of the main surface dynamics at the Balearic Basin scale. In order to quantify the absolute surface geostrophic currents, coastal altimetry-derived current computation was improved and cross-compared with its equivalent derived from glider measurements. Model simulations were then validated with the multi-sensor observations both qualitatively and statistically. The combined use of modelling and multi-sensor observing data reveals the baroclinic structure of the Balearic Current, the Northern Current and a small-scale anticyclonic eddy observed at North east of the Mallorca coast (current ~15cm/s, <30km in extent and > 180m deep). This mesoscale structure, partially intercepted by glider and along-track altimetric measurements, is marked by relative strong salinity gradients and not, as usual, by temperature gradients. Finally, the use of the validated model simulation also show that the geostrophic component of this small-scale eddy is controlled by sub-surface salinity gradients. We hypothesize that this structure contains recently modified Atlantic water arriving from the strait of Ibiza due to a northerly wind which strengthens the northward geostrophic circulation.

I·M·E·D·E·A
Institut Mediterrani d'Estudis Avançats

Jérôme Bouffard

Post-doctorant in Physical and Spatial Oceanography at IMEDEA (CSIC-UIB)[1]
C/Miquel Marquès, 21, 07190 Esporlès, Mallorca, SPAIN
Tel: +34 971 611 949
Mail: jerome.bouffard@uib.es

Cover Letter for the revised version of Bouffard et al.

Dear Editor,

Please find enclosed the revised version of our manuscript entitled "Sub-surface small scale eddy dynamics from multi-sensor observations and modelling" (PROOCE-D-11-00015) by Jérôme Bouffard, Lionel Renault, Simon Ruiz, Ananda Pascual, Clair Dufau and Joaquin Tintore, submitted to *Progress in Oceanography* after major revision.

We gratefully acknowledge you and the reviewers for their fruitful comments which we have used to restructure and fundamentally improve the paper. Please find enclosed the detailed answers and clarifications corresponding to the points specifically raised by each of the reviewers.

We hope that you will find that the enclosed manuscript is suitable for publication in *Progress in Oceanography*.

Sincerely yours,

Dr. Jérôme Bouffard

20/03/2012

[1] Now at Aix-Marseille Univ, MIO UMR 7294 (CNRS), 13288, Marseille France

==========
Reviewer #1

Recommendation: Reject

This manuscript is a descriptive jumble of topics, ideas, and methods without a clear central focus or hypothesis. While there are some nuggets of new and/or interesting information, the overall result is a superficial treatment of too many disparate topics. As such, I don't believe it meets the standards of Prog. Oceanogr. and should be rejected. I suggest the authors recast this manuscript into at least two separate and tightly focused contributions: one dealing with the observations, and a second with the remote sensing and numerical modeling. While there are comparisons to be made between these various methodologies, the present manuscript spends too much effort demonstrating that these data sources are useful (or similar, or complementary, or novel, etc.) and not enough effort discussing the underlying physics that motivate all of the measurements and data analysis. Besides the obvious length, I found the paper extremely difficult to read due to the lack of prior proofreading for proper English usage and grammar and the excessive use of non-standard abbreviations.

The co-author and I understand the reasons which led Reviewer#1 to reject the paper in its original form. We however believe that there are sufficient results for a publication adhering to the *Progress in. Oceanography* standards. Indeed, the major problem lay in the presentation of the results. After careful consideration, additional work and several meetings with the co-authors, **we have decided to entirely restructure the paper** by following the standard "Article structure" suggested by the *Progress in Oceanography* guide for authors:
http://www.elsevier.com/wps/find/journaldescription.cws_home/422/authorinstructions

Moreover, the paper has been almost fully rewritten with the help of a native English speaker and several new quantitative results have been added in order to better convince the reader (following suggestions made by reviewer #2). Also, the excessive technical and methodological aspects related to coastal altimetric and glider processing techniques have been reduced. This part was maybe not within the scope of *Progress in Oceanography,* and detracted from the principal messages of our study. In this respect, the study on glider and altimetric correction sensitivity will be used for another contribution to a more technical journal As suggested by reviwer#1, **the current paper has been re-focussed on the underlying physics**, throughout the full characterization of observed features in the Balearic Sea where the signal to noise ratio in observation is known to be particularly low. As a new result in the revised paper, we have been able to show that the geostrophic currents of an observed and simulated mesoscale structure were mainly driven by salinity gradients and not, as per usual in the Balearic Sea, by temperature gradients, which represents a major finding with respect to previous studies. We therefore demonstrate the key role of water mass exchanges and particularly salinity properties between the northern Gulf of Lions and the southern channels. Despite new scientific results and following the suggestion made by reviewer#1, the length of the manuscript has been reduced of about 20%. Moreover the number of non-standard abbreviation has been reduced (from 16 to 10 in the revised paper).

In accordance with the considerable effort made to improve our manuscript (both in terms of restructuration and new results), we hope that reviewer#1 will find this new version relevant for publication in *Progress in Oceanography*

==========

Reviewer #2

Review of PROOCE-D-11-00015

Recommendation: Major revision

Sub-surface small scale eddy dynamics from multi-sensor observations and modeling
Bouffard, Renault, Ruiz, Pascual, Dufau and Tintore

First of all, we would like to deeply acknowledge the relevant suggestions made by reviewer 2. We fully agree with the most of comments and have closely followed his/her pertinent recommendations in order to make the paper more in line with the *Progress in Oceanography* standards.

In this respect the paper has been deeply restructured in order to clarify the objectives and the major outcomes. For this, we have reorganized the revised manuscript following the standard "Article structure" suggested by the *Progress in Oceanography* guide for authors:
http://www.elsevier.com/wps/find/journaldescription.cws_home/422/authorinstructions

The paper has been almost fully rewritten in agreement with the 2 reviewers' comments and with the help of a native English speaker. Moreover, **numerous quantitative statistics have been added** (7 tables of statistics + Figure 4f + Figure 9f + Figure 10) whereas the technical aspects related to coastal altimetry methods/corrections have been reduced.

Although the conclusions and the material are essentially the same as in the first version, the paper has been completely restructured and it is now particularly complicated to find any correspondence (in term of section number, line numbers, Figure etc) with the former manuscript. We however did our best to address each point made by the reviewer and to provide detailed responses to his/her fruitful comments.

This paper presents an attempt to employ satellite remote sensing, glider-based observations and regional scale modeling (using ROMS) to characterize mesoscale and submesoscale features in coastal regions. The study focuses on the Balearic Sea, between the east coast of Spain and Mallorca, which has been the site of previous investigations undertaken by these authors. The bulk of the paper is devoted to presenting intercomparisons between dynamic height, current speed and, to a lesser extent, temperature and salinity derived from remote sensing, glider-based sections and models. These results are used to argue that the ROMS results accurately reproduce regional dynamics, after which the remainder of the paper uses the simulations to argue that 'submesoscale' features observed in model results and altimeter-derived surface geostrophic currents are driven by salinity gradients produced by the meeting of inflowing Atlantic waters and south-flowing Mediterranean waters. The paper's primary results are: (i) the use of glider-based measurements to evaluate altimeter-based surface geostrophic velocity estimates in a coastal region, (ii) application of altimeter-derived surface geostrophic currents to assess depth-average current estimates from gliders and

The scope of the revised manuscript is almost the same as the one addressed in the

first version. But the main objective is now clearly enounced in the introduction part:

"As a step forward, the present paper proposes to scientifically exploit such datasets in support of regional modeling, with the main objective (…)mesoscale structures" (line 121-127). And the way this objective is addressed is also clearly described: "The article is organized as follows (…) glider transect." (Lines 128-137)

The first part of the revised manuscript is closer to a cross-comparison between non-perfect observation systems rather than a quantitative "evaluation" of the corrections, methods and parameters used. Our main purpose is, by using several datasets, to increase our confidence in the interpretation of the observed patterns because over our study area, "the signal to noise ratio in observations is generally low" (line 163-167). The study of (sub)mesoscale therefore requires the use of several points of view (in-situ, remote sensing, modelling). Moreover, throughout the manuscript we highlight the limitations of each dataset, specifically in terms of resolution, coverage and synopticity which also justify the use of complimentary multi-sensor data. This aspect is also developed in the discussion section (line 693-724)

(iii) demonstration of a regional model's ability to reproduce the gross mesoscale features of the Balearic Sea.

In order to determine the model's ability to reproduce the gross mesoscale features, we have added numerous new diagnostics with well-defined standard metrics (See section 'Model validation').

The authors tackle the interesting and worthwhile problem of integrating in situ observations with remotely sensed altimetry. Given the disparate temporal and spatial scales of the various measurements, this is a difficult task. Accordingly, the paper focuses primarily on assessing the chosen approach by comparing dynamic height and current speed derived from remote sensing, gliders and models, though it bills itself as an examination of meso/sub-mesoscale eddy dynamics. A detailed presentation and evaluation of the techniques could have been a substantive contribution. Unfortunately, although a good deal of effort has clearly been invested in this study, the paper fails to achieve this. The study relies on highly qualitative comparisons rather than developing and employing quantitative approaches for assessing agreement between the various estimates and fields.

Indeed, the excessively qualitative comparisons provided in the first version may seem speculative. However, the new manuscript statistically quantifies the main conclusions which emerged from the previous manuscript. The revised manuscript therefore particularly focuses on quantitative comparisons between the various estimates and fields as suggested by reviewer 2. For this, we have used several statistical methods (temporal and spatial comparisons in terms of percentage of std explained, correlations, mean differences etc.). The differences in terms of physical contents, accuracy and sampling between the different datasets are also discussed throughout the manuscript. Direct quantitative comparisons between the model outputs and various in-situ and remote-sensed data are provided both at the Basin scale and over the specific area of the studied event (at surface and in the first 180 m depth).

The paper typically reports that remote sensing, glider-based observations and model results are 'in good agreement', without defining the criteria used for the comparison.

Examining the side-by side figures provided as evidence, the asserted agreement is sometimes less than obvious. Even the simplest measures, such as plots of the differences, were not

presented, and in some cases, comparisons were made between somewhat different quantities (relative geostrophic speed from one source against absolute geostrophic speed from another) when it would have been straightforward to compare identical quantities across the various sources. The assertions made throughout the paper would be far more credible if backed by quantitative comparisons of the field. I found the paper difficult to follow, with important gaps in information, sometimes vague or confusing explanations and some parts of the text that were clearly incorrect.

Given these issues and, most importantly, the fact the glider-altimeter-model comparisons that form the backbone of this work were inadequate, I cannot recommend that this paper be published in its current form. The study will require reworking at a fairly fundamental level to address these concerns.

These concerns are specifically addressed in the revised manuscript following the suggestions of reviewer 2

Concerning observations:

In section 411, satellite gridded altimetry and SST provide a first qualitative analysis of the surface patterns. However, in the following sections, new quantitative, statistics (table 2) are provided in order to compare surface Geostrophic current derived from gridded altimetry, PISTACH along-altimetry, glider and model. In addition to Figure 3, the results are also discussed in terms of correlation and mean differences (line 336-354, table 2). The potential non homogeneity between glider and altimetric currents in terms of synopticity and physical content is raised in “the material and method section” (lines 257-259) and also reminded in section 4.1.1: “despite the potential inconsistencies due to temporal lags between the (instantaneous) altimetric and non synoptic glider measurements” (lines 342-344).

Concerning Model:

In the revised manuscript, the model has been intensively validated both at the Balearic regional scale (with remote-sensing fields) during the July-August 2008 periods and also specifically during the glider mission, at surface and along the water column (with glider and PISTACH altimetric product). For this, an entire new section is now dedicated to the model validation (from line 420 to 621). Figure 5 allows a first spatial pattern comparisons with remote-sensing. In complement, new comparisons of the temporal variability of SST and EKE mean spatial average are also provided (time series and differences for EKE on Figure 6) in addition to table 4 which reports the main statistics (mean, std, absolute difference). Moreover we also complete it with new quantitative comparisons in Appendix A (refer to table A1, A2 and Figure A1,A2). These quantitative results are complementary to the more qualitative comparisons previously done. We also provide other quantitative comparisons in terms of surface accross-track Geostrophic current interpolated at the glider/altimetric track location (mean and correlation at northward and southward transect). The results in terms of relative current are reported on Table 6 whereas the results in terms of absolute currents are discussed in details in section 4.2.1.4 (lines 574 to 619).The signal along the water column has also been investigated by numerous new quantitative comparisons with glider measurements. The statistical results are summed-up on Figure 10 and throughout the associated interpretations done from line 533 to line 551.

Some specific comments follow below.

In general, the analysis relies too heavily on purely qualitative arguments, even in places where quantitative analyses would have been possible. For example, the paper often asserts that two fields (e.g. maps of altimeter-based and modeled geostrophic current) 'look' the same, with no attempt to define and calculate a quantitative metric to support this statement. These sorts of arguments are common throughout the paper.

Ok, see previous paragraph.

- Important details about the data are missing. For example, it was unclear to me whether the glider data were limited to only 2 occupations of the section ('go' and 'back') or whether there were multiple occupations. How long did it take gliders to traverse the section?

Concerning altimetry, we believe that table 1 and new references provided in the paper (ie PISTACH data Handbook, SSALTO-DUACS Handbook etc) are sufficient to satisfy the reader.

Concerning glider, numerous new details have been added in the revised manuscript about the data characteristics (horizontal and temporal sampling, corrections applied etc) and the current computation (lines 221-260). In particular, it is now clearly specified how long it takes the glider to complete its trajectory.

- Lines 323-326: “ In order to do this, the glider transects were almost co-localized with the JASON 2 altimetric track along a northward (period: 13/08/08 - 20/08/08) and southward (period: 21/08/08 - 27/08/08) transect (see Figure 1, for the glider transect location at northward transect, southward transect is almost the same) “
- line 370; ”northward transect, co-localized at surface with the altimetric track (results at southward transect, not shown here, are equivalent).”
- Also refer to the legend of Figure 1
- The glider transect position at time of northward measurements also appear on Figure 2, 5,7,8,16 and it is noted several times that the return transect (southward) has almost the same trajectory (that is the reason why it is not shown on figures)

- p6, 115: 'precise but sporadic'. Not sure what this is supposed to mean. Gliders are not at all precise in their navigation, and they are extremely slow-moving (they take a long time to cover any significant distance).

This possible confusing assertion has been removed. As noted previously, we have however specified the glider-derived absolute current is not really precise (especially because of the GPS-derived current). For example, we note in the lines 341-343: “This unrealistic bias is likely due to instrumental errors in the glider GPS positioning system and induced glider compass errors (Merckelbach et al., 2008)” and also in the discussion part: “Focused on the glider platform, the observed bias (…) more accurate measurement of glider heading. (lines 710-715). Moreover the problem of

non synopticity, due to the fact the glider is “extremely slow-moving”, is raised several times in the revised paper.

- p12, 282-283: The calculation of relative cross-track geostrophic current from glider-based density sections and thermal wind does not imply that cross-track current is negligible at the reference depth (here the bottom of the glider profile). The currents are defined as being relative to the current at some arbitrary reference depth.
Right, it is now rephrased as follows (lines 230-234): “Relative geostrophic currents can be estimated by the thermal wind equation, from the glider Dynamic Height (DH) obtained from temperature and salinity fields (see Ruiz et al., 2009b) with respect to an arbitrary reference depth which is here the maximum depth of glider measurements (in our case 180 m)” and where velocities have been reported to be weak (Ruiz et al., 2009b)

- p12, 287: Glider depth average velocity is typically estimated by differencing displacement predicted using a hydrodynamic model (with time series of glider heading, pitch, roll and buoyancy as inputs) from the actual displacement calculated using the GPS fixes at the start and end of each dive and dividing by dive duration.
Right, this is in agreement with the new descriptions done in lines 236-239: “with depth-averaged currents retrieved from the GPS glider positioning. These depth-averaged currents are obtained using a hydrodynamic model and based on the assumption that the main difference between glider GPS surfacing points and dead-reckoned positions is due to horizontal currents.”

- p12, 288: What is the 'vertical average CTD velocity'? Is this supposed to mean the vertically-averaged relative geostrophic cross-track velocity estimated by integrating the thermal wind equation?
Right, but this turn of phrase is not very standard. Thus, the use of “'vertical average CTD velocity'” has been removed.

Including the equations might help… the expressions for estimating absolute geostrophic cross-track velocity are:
This section has been clarified, in particular by adding the following equations, as suggested by reviewer 2 (However, as noted in the paper, the glider and altimetry current computation is also described in details in Bouffard et al., 2010).

$u_g(z) = u_{rg}(z) + u_{ref}$ [total geos velocity = relative + reference]

$u(z) = u_{rg}(z) + u_{ref} + u_{ag}(z)$ [obs velocity = rel. geos + reference + ageos]

$u_{ref} = \langle u(z) \rangle - \langle u_{rg}(z) \rangle - \langle u_{ag}(z) \rangle$

$u_g(z) = u_{rg}(z) + \langle u(z) \rangle - \langle u_{rg}(z) \rangle - \langle u_{ag}(z) \rangle$

$\langle\rangle$ = vertical average

$u(z)$ = obs velocity, such that $\langle u(z) \rangle$ is the glider-based depth-average velocity

$u_g(z)$ = absolute geos velocity

u_rg(z) = relative geos velocity (from thermal wind)

u_ref = reference geos velocity

u_ag(z) = ageostrophic velocity

- p13, 296-304: Glider heading errors typically depend on heading, pitch and roll, and are rarely a uniform offset. Glider compass calibration typically involves collecting data at a representative set of heading-pith-roll combinations and then using these in a model to generate corrected coefficients for the glider compass. Calibration at a single pitch-roll combination (flat) is likely to be inadequate.
We believe that, in our case, such an error can effectively be considered as an offset given the relatively short length of our glider transect (only few tens km). But we agree with reviewer 2 that our compass calibration experiment was not robust enough to provide a "valid compass correction". This part has been therefore removed in the new manuscript since this does not constitute the main scope of our study.. This would require further investigation, as it is noted in the discussion section: "In particular, we would expect to achieve better results with a more accurate estimation of the error in the glider displacement assumptions which imply more accurate measurements of glider heading" (lines 713-715).

- p16, 385-386: 'general good agreement' in Fig. 2. What is the metric used to make this assessment? Could we see a plot of the difference between the ROMS and altimeter maps? Except at the broadest scale, the maps do not look all that similar to me. That said, I do not know what the criteria the authors used to make this assessment.
We are not sure that difference of two maps would provide more relevant information than direct qualitative comparisons between the original maps. This is especially true when we look at (sub)mesoscale signals for which a small spatial lag of a few km could entail a strong disagreement and artificial features which would be difficult to interpret (even if the physical structures were quite equivalent in terms of size, shape and magnitude). This is why qualitative comparisons between non-perfect observations (as gridded altimetry: problem of MDT, smoothing effect of the OI etc…) and a model are also needed to assess the model ability to reproduce the main dynamical patterns (even if they are not exactly at the right time and at the right place). However, in order to give weight and robustness to such qualitative analysis, several efforts have also been made in order to provide quantitative diagnostics, both in terms of mean spatial fields but also in terms of temporal evolution of surface EKE and temperature (see 'Model validation' section). This has been done not only at the domain scale but also by dividing the domain in several areas to evaluate the space/time differences between model and remote-sensing (Appendix A).

- p17, 404-406: I don't understand this statement. The paper states that, other than the two obvious strong currents, there are no significant mean flows in the glider section, and suggests that this is due to 'high-frequency instable and partially ageostrophic small-scale structures'. However, does it make sense to talk about the altimeter-based surface velocities as estimates of the mean currents? And if I understand the glider data correctly, there are only two sections, making it pretty much impossible to formulate a sensible mean. This leaves only the model results, and here it should have been possible to determine the variance in such high-

frequency motions and whether there is a background mean flow that they actually mask.
Here, we dealt with altimetric spatial mean (and not temporal mean …)

- p17, 419: Again, it would have been useful to define the metric (hopefully something quantitative) behind the 'very good agreement' statement and then back the statement with some actual analysis.
Right, see above

- Fig. 3: Why not plot altimeter-based absolute geostrophic surface current vectors over the AVHRR SST maps? This would provide a depiction parallel to that on the left side (ROMS SST and velocity).
Done, in the revised version (refer to Figure 2 and Figure 7)

- Fig. 4: Perhaps I'm misreading this, but it seems that there are different current vectors plotted in the two ROMS panels (left side, top & bottom).
This Figure no longer exists in the revised paper

- p18, 431: SST cannot become fresher… perhaps ' … SST cools over the entire domain …'.
Right, this expression has been modified

- p19, 454 and Fig. 4: 'agreement between ROMS and gridded altimetry is improved…'. Improved relative to what? What metric, and how measured?
This sentence has also been removed given that it was purely qualitative and maybe confusing. The main message was that the MDT can have damaging impacts. Thus, when its impact is removed the agreement between model and gridded altimetry could be improved over some areas. In the revised manuscript, qualitative and quantitative analysis confirm this. Figure 8 clearly shows evidence of good qualitative agreement between the two maps when the MDT effects are avoided. Even if no statistical metrics are used here, it is clear that the main features are reproduced by the model. Moreover, the damaging impact of MDT is also confirmed through quantitative analysis in terms of EKE (refer to table 4 and table A2) and discussed throughout the paper and appendix as potential limitation of gridded altimetric products.

-p19, 461: 'SST variability is marked by a general decrease'. SST variability does not decrease (or at least the figures do not reflect this), but the region does appear to cool.
Thanks, the sentence has been reformulate accordingly: “The SST cools throughout the western part of the domain, where a mean decrease of 1.5°C is observed, with reference to the previous 15 days” (line 309-310)

- p19, 467-468: the text says total surface current, but the Fir. 4 caption states that the vectors are current differences.
This Figure has been removed in the revised paper

- Fig 4 caption, 877: '… mission (top) …' should read '…mission (bottom) …'.
This Figure has been removed in the revised paper

- p21, 503: Why not use the estimate of glider u_ref here?
Correct, but we have removed this sentence from the manuscript.

- p21, 505: '… negative slope of about 8 cm …'. This is not a slope, it is a drop in dynamic height. Need to divide by distance to calculate the slope…
The references to dynamic heights (and therefore this sentence) have also been removed in the revised manuscript

- p21, 509-516: Regarding stated good agreement between glider and altimeter absolute geos current, again there is no stated metric. I agree that 'go' looks closer the 'back', but even for 'go' the glider sits outside one STD for the altimeter values, and back has clear biases (which the authors note). Why was there no attempt to form a statistical comparison?
We are a bit surprised by this comment given that, in the former paper all these statistics were provided in table 3 (as noted in line 510 of the former manuscript). Our text was maybe not sufficiently clear and led the reviewer#2 to some misunderstanding. Equivalent statistics (but in terms of mean and correlation) are also provided in table 2 of the revised paper with, hopefully, clearer explanations.

- p23, 581: The stated numbers do not appear in the referenced table (Table 5).
This part has been removed in the revised paper.

For clarification: the stated numbers did not appear in table 5 (of the former manuscript) because they simply correspond to the reduction of altimetry –glider mean differences whether or not we use the compass correction (hereafter "CC"):
line 1-line 2= 3,3 cm/s (without CC)-2,5cm/s (with CC)=0,8cm/s
Line 3-line 4= 12,8cm/s (without CC) -8,3cm/s (with CC)=4.2 cm/s

As noted in line 581, we wanted to show that CC "reduces the altimetry to glider difference"

- Table 5 & 6: Contents of these tables are poorly explained in the body text and caption.
Perhaps this is why some of the statistical interpretation (above) was not very clear.

- p24/25, section 3.2.4: Why are glider and ROMS relative geostrophic currents being compared to altimetric absolute geostrophic currents here? Is there a reason to base this section on a comparison of related, but dissimilar, quantities? This obfuscates the comparison. Later in the section the fact that absolute and relative currents could even be of differing signs depending on the reference is used to argue the importance of subsurface measurements, but this should not be news to anyone.
It was effectively to argue the importance of subsurface measurements. But we agree with reviewer 2 that it was not relevant. Therefore, this comparison between relative and absolute current has been removed in the revised version. However we provide direct comparisons between model and glider relative geostropic current in order to evaluate the model's performance (avoiding therefore error from glider GPS-derived current).

- p25, 611-614: This argument does not explain the differences between model and altimetric currents.
Right, removed in the revised manuscript

- p26, 644-645: More '… in very good agreement…' statements without metrics or actual

backing. Due to the way the data are plotted, I cannot assess, even qualitatively, how well the two fields agree. I suspect that the vertical temperature structure differs a bit, and salinity fields show clear differences. Some of the wiggles in the glider sections may be due to internal wave heaving, but this is not enough to explain the obvious differences.
We thank the reviewer#2 for this valuable comment. In complement, quantitative statistical comparisons between model and glider (S, T and density function of depth) are thus provided on Figure 10 of the revised paper. The related analysis is done between lines 534-552. As suggested, we also refer to internal wave :"Moreover, the glider section show some wiggles in the first layer that may be due to internal wave heaving that are not reproduced by the model" (lines 532-533).

It would have been useful to see potential density sections, and to understand the relative roles of heat and salt in setting density in this particular region.
The potential density section from glider and model has been added (Figure 4c and 9c). Moreover statistical comparison between glider and model density profiles are now provided on Figure 10 (see previously)

- p26, 652-653: Text states that salinity gradients are perfectly phased with altimetric and glider-based absolute geostrophic currents, but not evidence is shown. It would be useful to see a plot.
We do not provide a plot but 2 tables (table 3 and table 5) that confirm this assessment both for model output and glider are included.

-p26, 659+: Paper has not demonstrated that density is controlled by salinity. Is this true even at depth? The glider profiles do not extend very deep…
We thank reviewer 2 for this relevant comment. Indeed, the study of the relative role of heat and salt in setting density is maybe one of the major improvements in the new manuscript. We have proposed a demonstration that clearly shows (quantitatively) geostrophy is controlled by the salinity gradient (both in the model and observations), at least below 60m and 100m depth for respectively the glider and model (for glider: refer to lines 386-406 and for model: refer to lines 554-563)

- p28, 680-688: Stated good agreement between ROMS and glider-based velocity sections is not completely obvious, even if we allow for a spatial offset. Vertical structures and lateral extents differ.
As notes previously, Figure 10 provides new statistics of temperature, salinity and density profiles (from which the across-track Geostrophic current is derived). The observed spatial offsets are also noted in the revised manuscript.

- Fig 9. Caption refers to (a) and (c) but not to (b).
Right, but this Figure and the associated caption have been modified in the revised paper

- p28, 702-708: Need to build a stronger case to support the statement that altimeter and glider results demonstrate that the model can reproduce the dynamics.

We agree that we have to be careful with such statements but the new statistical comparisons with several independent data (with satellite SST, gridded altimetry EKE, along-track altimetric currents and glider hydrographic fields) should allow us to affirm, a least, "our major but realistic hypothesis is that the same kind of structure has been intercepted by the glider and along-track altimetry measurements".

Moreover, the new quantitative results showing that the relative role of salinity and temperature in the geostrophic current are similar in model and glider (see previously and particularly tables 3, 5; Figures 4f, 9f) also provide a strong argument on the model's ability to reproduce the observed dynamics.

- p30, 749-750: Unclear how 'multiple-sensor data' identified these boxes as special places. Needs some explanation.
Even the boxes are chosen empirically (function the observed dynamics at the Balearic scale), this has been clarified in the revised paper (lines 623-629): "Three virtual boxes are located at critical places chosen with respect to the previous analyses done with the multi-sensor data and oceanic model outputs (…) (blue box in Figure 7, b).

- p30, 753-754: Blue box is actually west of ASTERIX.
Right, corrected in the revised manuscript

- p30, 759-761: I'm not sure the statement about time evolution applies here, as the data do not really address this.
This diagram (now on Figure 13) has been done with (T,S) variables available for the whole July-August time period. They are spatially averaged (in each box) but not time averaged. Thus, more points' dispersion (red dots on Figure 13) means more hydrologic changes of water-masses. As noted in line 636 of the revised paper (and also clearly confirmed for salinity on Figure14a, top-left) this "suggests a progressive change of water masses properties during the 2 month study period". For clarification we have added in the associated legend "spatially-averaged (but not time averaged) for each of the 3 boxes"

- Although I appreciated the list of acronyms at the start of the paper, the extensive use of these abbreviations (and others that are not in the table) made the paper more difficult to read than it needed to be. Perhaps it'd be better to choose a much smaller set of acronyms and spell out the rest of the words.
The list of acronyms has been strongly reduced, (from 16 to 10 elements). Moreover, the use of acronyms has been entirely avoided in the discussion-conclusion section.

***Highlights (for review)**

We study horizontal flows associated with the regional oceanic mesoscale in the Balearic Sub-basin> Glider measurements, remote-sensing data and a regional oceanic model are used conjointly > Model and multi-sensor cross-comparisons show good agreements in surface and depth> Their combine use allow to characterize small-scale eddies and explain their formations.

Sub-surface mall-scale eddy dynamics from multi-sensor observations and modelling

J. Bouffard[1, 2], L. Renault[1, 3], S. Ruiz[1], A. Pascual[1], C. Dufau[4], J. Tintoré[1,3]

Submitted to *Progress in Oceanography*

[1] *IMEDEA (CSIC-UIB), TMOOS Dept, Mallorca, Spain*

[2] *Now at Aix-Marseille Univ, MIO UMR 7294 (CNRS), 13288, Marseille France,*

[3]*SOCIB, Coastal Ocean Observing and Forecasting System, Spain*

[4]*CLS Space Oceanography Division, Ramonville, France*

Corresponding author:

Dr. Jérôme Bouffard

IMEDEA (CSIC-UIB)

C/ Miquel Marquès, 21 07190, Esporles, SPAIN

Now at Aix-Marseille Univ, MIO UMR 7294 (CNRS), 13288, Marseille France

E-mail: jerome.bouffard@uib.es and/or jerome.bouffard@univ-amu.fr

Key words: mesoscale eddy, multi-sensor, coastal altimetry, glider, regional modelling

Abstract

The study of mesoscale and submesoscale [hereafter *(sub)mesoscale*] hydrodynamic features are essential for understanding heat and biogeochemical exchanges between the coastal and open ocean. In this context, a glider mission was carried out in August 2008, well co-localized and almost simultaneously with a JASON 2 altimetric pass in order to fully characterize currents associated with regional (sub)meso-scale processes regularly observed to the north of Mallorca (Mediterranean Sea). A synoptic view from satellite remote-sensing fields, before and during the glider mission, provided a descriptive picture of the main surface dynamics at the Balearic Basin scale. In order to quantify the absolute surface geostrophic currents, coastal altimetry-derived current computation was improved and cross-compared with its equivalent derived from glider measurements. Model simulations were then validated with the multi-sensor observations both qualitatively and statistically. The combined use of modelling and multi-sensor observing data reveals the baroclinic structure of the Balearic Current, the Northern Current and a small-scale anticyclonic eddy observed at North east of the Mallorca coast (current ~15cm/s, <30km in extent and > 180m deep). This mesoscale structure, partially intercepted by glider and along-track altimetric measurements, is marked by relative strong salinity gradients and not, as usual, by temperature gradients. Finally, the use of the validated model simulation also show that the geostrophic component of this small-scale eddy is controlled by sub-surface salinity gradients. We hypothesize that this structure contains recently modified Atlantic water arriving from the strait of Ibiza due to a northerly wind which strengthens the northward geostrophic circulation.

Acronyms

BC	Balearic Current
Corr	Correlation with statistical significance > 95 %
DH	Dynamic Height derived from the glider CTD
IGDR	Interim Geophysical Data Record
MDT	Mean Dynamic Topography
(M)SLA	Map of Sea Level Anomaly
NC	Northern Current
SLA	Sea Level Anomaly
STD	STandard Deviation
SWOT	Surface Water and Ocean Topography

Plan

1. Introduction

Mesoscale and submesoscale hydrodynamic features are particularly important to establish and understand the horizontal and vertical transport of heat (Volkov et al., 2008) and biogeochemical tracers (McGillicuddy et al., 1998; Levy, 2008 and references therein). Indeed, 90% of the kinetic energy of ocean circulation is contained in small-scale features (e.g. eddies, fronts, filaments) whereas 50 % of the vertical exchange of water mass properties between the upper and the deep ocean may take place at the (sub)mesoscale (Fu et al., 2010a, 2010b). The challenge of extending our knowledge on the formation, evolution and dissipation of eddy variability is therefore critical to understanding the ocean's roles in Earth's climate. This highlights the importance of describing complex ocean dynamics from a theoretical and modelling point of view (Klein and Lapeyre, 2009; Capet al., 2008a 2008b, 2008c; Hu et al., 2009) but also using observational approaches adapted to the coastal domain (Nencioli et al., 2010; Bouffard et al., 2010; Hu et al., 2011; Garreau et al., 2011).

Eddy signatures in terms of sea surface height have revealed that multi-satellite altimetry is highly effective in observing and tracking eddies in the global ocean as they provide almost synoptic and periodic measurements of the sea surface topography (Chelton et al., 2011; Le Morrow and Le Traon, 2011). However, given their relative limited resolution, the single use of standard geostrophic current maps derived from multi-satellite altimetry (Ducet et al., 2000) is not always sufficient in order to characterize the spatial and temporal variability of (sub)mesoscale features at coastal and regional scales (Dussurget at al., 2011). Sea surface properties related to geostrophic and ageostrophic (sub)mesoscale motions are clearly observed on satellite sea surface temperature and ocean colour images (Lehan et al., 2007) but such surface signatures do not convey much quantitative information on associated currents and sub-surface structures. In addition, the relatively sparse distribution of conventional *in-situ* measurements at depth (such as ADCP, Argo floats, etc) and at the surface (such as drifters) only provide limited quantification of (sub)mesoscale processes and associated mechanisms along the water column.

In this context, complementary high resolution monitoring technologies (e.g. autonomous underwater vehicles or gliders) are also being implemented in ocean observatories such as; IMOS in Australia[1], OOI in the USA[2], and in Europe SOCIB[3] and MOOSE (Mediterraneen Ocean Observing Site for Environment). By collecting high resolution observations of temperature, salinity and also biogeochemical variables both at the surface and through the water column, gliders lead to major advances in the understanding of key scientific questions related to (sub)mesoscale physical and biogeochemical processes (e.g. Sackmann et al., 2008; Niewiadomska et al., 2008; Perry et al., 2008; Martin et al., 2009a; 2009b; Hodges and Fratantoni, 2009; Testor et al., 2010).

Moreover, numerous studies have indicated additional benefits when gliders are combined with altimetry to monitor transports (Gourdeau et al., 2008) and to characterize mesoscale structures in the upper ocean (Hátún et al., 2007; Martin et al., 2009a,2009b; Ruiz et al., 2009a, 2009b; Pascual et al., 2010). Bouffard et al (2010) recently developed innovative strategies combining improved coastal along-track altimetry (rather than standard altimetric maps) and glider data to more precisely quantify horizontal flows, specifically in terms of current velocity associated with filaments, eddies or shelf-slope flow modifications in the Balearic Sea. The use of these two datasets improves the separation of small-scale dynamics from noise. This has revealed the presence of relatively intense eddies as previously observed with satellite infra-red images and *in-situ* data confirming that (sub)mesoscale variability is a dominant factor affecting the local circulation and water exchanges between the Balearic adjacent sub-basins (Pinot et al., 1995). As a step forward, the present paper proposes to scientifically exploit such datasets in support of regional modeling, with the main objective of improving the characterization of small mesoscale features as well as investigating the formation process and associated forcing. The study area is the Balearic Basin (Figure 1), located in the Western Mediterranean where the

[1] http://www.imos.org.au
[2] http://www.oceanleadership.org/programs-and-partnerships/ocean-observing/ooi/
[3] http://www.socib.es/

circulation is rather complex due to the presence of multiple interacting scales, including basin, sub-basin scale and mesoscale structures.

The article is organized as follows: firstly we briefly present the study area characteristics. Secondly, we describe the experimental coastal altimetric data, the glider data and the model configuration used. After this, we proceed to a description of dynamical patterns observed in August 2008 from multi-sensor data both at the Balearic Basin scale (with remote-sensed Sea Surface Temperature and atimetric current maps) and north of the Mallorcan coast (with glider and along-track altimetry observations). The results obtained from the multi-sensor dataset will be then compared to a realistic numerical simulation, at the surface and along the water column. Finally, the validated simulation will be exploited to identify the potential mechanisms associated with the small-scale structure simulated north of Mallorca and also previously observed along the altimetric and the glider transect.

2. Study area

The general surface circulation of the Balearic Sea is mainly controlled by the presence of two fronts and their associated currents (Font et al. 1988; Font, 1990). The Catalan front is a shelf/slope front that separates old Atlantic Water (AW), in the center of the Balearic sub-basin, from the less dense water transported by the Northern Current (NC), which is also old AW but fed in the Gulf of Lions and the Catalan shelves by continental fresh water (refer to Figure 1). The NC is a density coastal current flowing southwestwards, in a cyclonic way, from the Ligurian Sea to the Balearic Sea. There, it passes the Ibiza channel or retroflects cyclonically over the insular slope forming the Balearic Current (BC). The Balearic front is also a slope front related to the presence of more recent modified AW that has entered the basin through the channels at south (La Violette et al., 1990). Both BC and NC have widths of the order 50 km and are in good geostrophic balance as winds only seem to produce transient perturbations in terms of near-inertial oscillations (Font, 1990). Beside the general basin scale circulation, the Balearic sub-basin is also characterized by frontal dynamics near

153 the slope areas and developing in between the BC and the NC, such as mesoscale eddies
154 (Tintoré et al. 1990, Pinot et al. 2002; Rubio et al. 2009), filaments and shelf-slope flow
155 modifications (Wang et al., 1988; La Violette et al. 1990). These have been found to modify,
156 not only the local dynamics, with associated significant vertical motions (Pascual et al. 2004),
157 but also the large scale patterns, as shown by Pascual et al (2002), in a detailed study of the
158 blocking effect of a large anti-cyclonic eddy. The submarine topography associated with
159 these complex interactions between the surface and subsurface waters plays a key role in
160 controlling the transport between the northern and southern regions (Astraldi et al., 1999)
161 and also may enhance the (sub)mesoscale activity in the Balearic Sea (Alvarez et al., 1996).

162 **Figure 1**

163 Despite several previous studies, the characterization of (sub)mesoscale dynamics in the
164 Balearic Sea is difficult given the wide spectrum of temporal and spatial variability of
165 processes with which they interact. Moreover the signal to noise ratio in observations is
166 generally low because the eddy kinetic energy over this area (Pascual et al., 2007) is around
167 ten times weaker than that observed by altimetry in the global ocean (Pascual et al., 2006).
168

169 # 3. Material and Methods

170 Due to the scales of wavelengths and magnitudes involved (few centimeters over few tens of
171 kilometres in terms of sea surface height); it is very difficult to differentiate small scale
172 dynamic features from noise in sea surface observations, specifically over the coastal
173 domain of the north western Mediterranean Sea (Bouffard et al., 2008; 2011). Cross-
174 comparisons between model and multi-source datasets should therefore increase confidence
175 in our dynamical structure characterization. Within this framework, a glider mission was
176 carried out, well co-localized and almost simultaneously with a JASON 2 satellite pass (see
177 Figure 1, right) with the main objective to characterize 3D horizontal currents associated with
178 the oceanic small mesoscale features. In addition to a more robust error budget assessment,
179 using both *in-situ*, remote-sensing and model has the advantage of providing complementary

information in terms of resolution (glider, along-track altimetry) and coverage (gridded altimetry, model). The next sections give a detailed description of the dataset and the model used.

3.1 Satellite altimetry

Radar altimetry is a key component for observing the open ocean circulation complexity (Le Traon and Morrow, 2001). However, coastal and regional dynamics in the Balearic sea, where horizontal spatial scales can be of the order of 10 km (Send et al., 1999), are much more complex to observe with altimetry. Until recently, along-track data had difficulties capturing the dynamics associated with coastal small scale processes, because the signal-to-noise ratio in the coastal band is rapidly degraded, as the altimeter and radiometer signals are perturbed at a 10 and 50 km distance to the coast, respectively. Apart from land contamination, data quality in these regions was due to a lack of coastal zone algorithms (Anzenhofer et al., 1999; Vignudelli et al., 2005).

In this respect, new altimetric post-processing methods and quality control procedures have been developed and can now be exploited for regional and coastal applications (Emery et al., 2011, Kouraev, 2011; Ginzburg et al., 2011; Lebedev et al., 2011; Bouffard et al., 2008, 2010, 2011, Roblou et al., 2011, Birol et al., 2010). These studies indicate that new strategies such as the use of high frequency along-track sampling (20Hz data), combined with a coastal-oriented editing strategy, better constrain the surface geostrophic current computation in the coastal domain and for dynamical structures smaller than 50 km.

In the present study, the post-processing of the coastal altimeter Sea Level Anomaly (SLA) is thus similar to that used in Bouffard et al. (2010) for ENVISAT, but applied to the JASON 2 experimental along-track data provided by the PISTACH project (see Table 1 for a summary of the main characteristics). Across-track altimetric geostrophic current anomalies have been then derived from fully corrected altimetric SLA. The along-track altimetric gradient is

estimated by using the optimal filter developed by Powell and Leben (2004) with a spatial window of 15 km which is about the first Rossby radius in the Mediterranean Sea (Send et al., 1999). The across-track surface geostrophic current is then calculated by adding the interpolated Mean Dynamic Topography (MDT) of Rio et al. (2007). By construction, this current is perpendicular to the satellite track that, in this case, intercepts the main components of dynamics related the BC and/or NC systems (see Figure 1). This kind of measurement will therefore be used in order to precisely quantify the surface geostrophic current intensity associated with the observed coastal and (sub-)mesoscale patterns.

Table 1

In complement, 2D surface geostrophic current derived from regional AVISO Maps of Sea Level Anomalies ((M)SLA on a 1/8° x 1/8° grid, Updated delayed-time product, ref. to SSALTO/DUACS User Handbook) added to the MDT will be also used in order to identify the main surface dynamic structures and provide a qualitative assessment of the model simulation at the Balearic Basin scale.

3.2 Coastal glider

In complement to altimetric observations, glider subsurface measurements will show the baroclinic structure of related surface patterns. In order to do this, the glider transects were almost co-localized with the JASON 2 altimetric track along a northward (period: 13/08/08 - 20/08/08) and southward (period: 21/08/08 - 27/08/08) transect (see Figure 1, for the glider transect location at northward transect, southward transect is almost the same),

The coastal glider has provided high-resolution hydrographic data between 10 and 180 m depth at about 500 m horizontal resolution. The glider data processing includes the thermal lag correction (Garau et al., 2011) for unpumped CTD sensors installed on Slocum gliders. Hydrographic profiles have been averaged vertically to 1 m bins. Relative geostrophic currents can be estimated by the thermal wind equation, from the glider Dynamic Height (DH) obtained from temperature and salinity fields (see Ruiz et al., 2009b) with respect to an

arbitrary reference depth which is here the maximum depth of glider measurements (in our case 180 m). The issue of reference level correction has been recently addressed in Bouffard et al. (2010) and Gourdeau et al (2008) and applied here by combining the relative geostrophic currents with depth-averaged currents retrieved from the GPS glider positioning. These depth-averaged currents are obtained using a hydrodynamic model and based on the assumption that the main difference between glider GPS surfacing points and dead-reckoned positions is due to horizontal currents. So, the difference between the relative depth-average geostrophic currents (from DH) and the absolute depth-average currents (from GPS glider positioning) should approximately correspond to the absolute geostrophic current at 180 m, since horizontal ageostrophic motion, tide currents, and barotrophic high frequency contributions can be considered as negligible (Bouffard et al. 2010). By adding this value to the relative geostrophic current at each depth level, absolute geostrophic current both at surface and along the whole 180 m water column can therefore be estimated as expressed in the following equations:

$$u_g(z) = u_{rg}(z) + u_{ref} \quad \text{Eq. (1)}$$

$$u(z) = u_{rg}(z) + u_{ref} + u_{ag}(z) \quad \text{Eq.(2)}$$

With u which corresponds to the total current at depth z (such that $\overline{u(z)}$ is the glider-based depth-average velocity), u_{rg} and u_{ag} are respectively the relative geostrophic and ageostrophic currents and u_{ref} the unknown current at the reference level depth.

By vertically averaging and combining Eq (1) and Eq(2) we obtain:

$$u_{ref} = \overline{u(z)} - \overline{u_{rg}(z)} - \overline{u_{ag}(z)} \quad \text{Eq.(3)}$$

Since the vertical average of horizontal ageostrophic motion is considered here to be negligible compared to total horizontal currents, we obtain from Eq (1) and Eq (3) the absolute geostrophic current from the sea surface to the reference level depth:

$$u_g(z) \approx u_{rg}(z) + \overline{u(z)} - \overline{u_{rg}(z)} \quad (4)$$

At the surface (for $z=0$) and setting aside the issue of synopticity, this quantity should be therefore directly comparable with the instantaneous co-localized absolute geostrophic current derived from altimetric measurements (when a MDT is also used)

3.3 Model description

The coastal and (sub)mesoscale processes north of Mallorca should be partially observed by the glider and along-track altimetric measurements, but they are space-time sub-sampled by these two observing systems. The interpretation of such data does not allow for a complete identification of mechanisms and forcings associated to the observed patterns. This is the main reason why a regional oceanic model has also been used in order to better characterize the water masses' dynamical interactions at the Balearic Basin scale and their relative positions with respect to the glider and altimetric track .

The oceanic model used is the Regional Ocean Modeling System (ROMS) (Haidvogel et al., 2000; Shchepetkin and McWilliams, 2005), a 3D free-surface, sigma coordinate, split-explicit equation model with Boussinesq and hydrostatic approximation. The reader is referred to the work of Shchepetkin and McWilliams (2005) for a more complete description of the numerical code. Note that the simulation has been implemented over the Balearic Sea and developed within the framework of the Balearic Islands Coastal Observing and Forecasting System (SOCIB, www.socib.eu and Tintore et al., 2012) and therefore is not specifically designed for the present study. The model domain extends from 1°W to 5°E and from 38°N to 44°N (see Figure 1b). The vertical discretization considers 30 sigma levels and the horizontal grid is 192 × 224 points with a resolution of 1km, which allows a good sampling of the first baroclinic Rossby radius of deformation throughout the whole area (10-15km, Send et al 1999). Bottom topography is derived from the Smith and Sandwell (1997). The simulation, lasting 2 years, is initialized on 1st May 2007 using temperature, salinity, horizontal velocities, and sea surface elevation derived from the Mediterranean Forecasting System (MFS, Pinardi et al., 2003). At the three laterals open boundaries (North, East and

South) an active, implicit, upstream biased, radiation condition connects the model solution to the surrounding ocean (Marchesiello et al., 2001). The daily MFS fields are used to infer the thermodynamics and the currents at the open boundaries conditions. Note that the connection between the MFS fields and the model did not create artificial features, therefore we can focus on features situated close the open boundary conditions. The regional configuration of the atmospheric model Weather Research and Forecasting (WRF, Skamarock et al., 2008) described in Ruiz et al. (2012), provides ROMS with the following atmospheric fields every 1 hour: 2-m air temperature, relative humidity, surface wind vector, net shortwave and downwelling, long wave fluxes, and precipitation. A bulk formulate based on Fairall et al. (2003) is used to compute turbulent heat and momentum fluxes.

4. Results

4.1 Hydrodynamics from observations

4.1.1 Synoptic view from remote sensing

Figure 2

Before the glider mission, from 01/08/2008 to 12/08/2008 (Figure 2, a) the AVHRR SST show a warm and relatively homogenous temperature of about 27 - 28°C in the centre of the domain whereas cooler water, less than 26.5 °C, is only present to the north and south. This is a typical configuration as described in section 2. Indeed, a marked temperature front, corresponding to the Catalan front is positioned to the north of the domain, separating colder (by 1.5°C) northern water from the warmer water of the Balearic Sea. This front (red dashed line on Figure 2,a) is remarkably well co-localised with the main surface absolute geostrophic current patterns derived altimetry sea level elevation (see vectors).

During the glider mission, from 13/08/2008 to 27/08/2008 (Figure 2, b), the synoptic situation becomes quite different. The SST cools throughout the western part of the domain, where a mean decrease of 1.5°C is observed, with reference to the previous 15 days. The map also

311 indicates a northward current flowing through the Ibiza Channel into the Balearic Basin along
312 the temperature fronts (red dashed line); one branch of this geostrophic flow propagates
313 north until 41°N, whereas another branch generates a meander after flowing along the north
314 coast of Ibiza. This meander expands at the time of the glider mission and evolves in an
315 anticyclonic mesoscale eddy (herafter called “OBELIX”, black arrow on Figure 2, b) with a
316 mean current of ~ 15 cm/s, centred southwest of the glider transect (2°E, 40.5°N). This
317 mesoscale structure is located at the interface between the relatively warm water to the
318 south and the cooler water to the north. It corresponds to the north-western border of the
319 new temperature front replacing the Catalan front previously observed (Figure 2, a). A branch
320 of the eastern border of this eddy partially feeds the BC which flows and accelerates
321 northward along the coast of Mallorca until the glider transect, at its south edge (near the
322 Minorcan coast). Farther north (>40.5 °N along the glider transect), apart from the return
323 branch of the NC located at the northern edge of the glider transect (also refer to Figure 1),
324 no clear sea surface signature is observed. .

325

326 **4.1.2 Surface currents from along-track altimetry and glider measurements**

327 Figure 3 shows absolute across-track surface geostrophic currents derived from glider,
328 satellite altimetry (both gridded and along-track product) and model (used later, in section
329 4.2.2.2) in order to precisely identify surface signatures associated with dynamical features
330 during the glider mission.

331 **Figure 3**

332 The northward (southward) glider transects, corresponding to the 13/08/08 - 20/08/08
333 (21/08/08 - 27/08/08) period, were compared with across-track altimetric measurements of
334 J2 cycle 4: 13/08/2008 (J2 cycle 5: 23/08/2008). The two measurements are spatially well
335 co-localized (Figure 1; right), but the time delay between instantaneous altimetry sampling
336 and glider could be a potential source of differences that have to be considered (not
337 specifically discussed here). Despite this, the correlations are of 0.91 and 0.73 respectively

for northward and southward transects (see Table 2). However, even if the spatial variations of current are well phased, an important bias (8.2 cm/s) is observed on the southward transect. This is not the case during the northward transect where the mean difference is only of 2.3 cm/s (Figure 3, b and Table 2). This unrealistic bias is likely due to instrumental errors in the glider GPS positioning system and induced glider compass errors (Merckelbach et al., 2008). To correct this, the spatial average altimetric absolute surface geostrophic current could be used as a reference, despite the potential inconsistencies due to temporal lags between the (instantaneous) altimetric and non synoptic glider measurements.

As in Bouffard et al. 2010 (for ENVISAT), comparisons also made with standard 1 Hz altimetry (not shown here) confirm that PISTACH 20 Hz along-track sampling using the new editing strategy (described in details in Bouffard et al., 2010) improve the altimetry - glider statistical consistency: at northward transect, correlations are 0.90 (for edited 20 Hz data) and 0.78 (for standard 1Hz data), with the percentage of STD explained of 55% (for edited 20 Hz data) and 35% (for standard 1Hz data). The same conclusions are obtained when glider surface absolute current are compared with the corresponding currents derived from standard AVISO (M)SLA. Despite weaker current amplitudes, this product (see grey curves on Figure 3) provides realistic surface currents when qualitatively compared to glider and along-track altimetry .

Table 2

The previous comparisons show a relatively good agreement (see Figure 3 and table 2) between glider and PISTACH along altimetry with current of about 15 cm/s at the south edge of the track. This would correspond to the BC position (see Figure 1 and Figure 2) whereas at the opposite edge, the two datasets also captured major dynamical features (currents > 10 cm/s) which may correspond to a return branch of the NC (see Figure 1 and Figure 2). In between the potential positions of the BC and NC, a small-scale oscillation is also revealed (hereafter called “ASTERIX”) whereas it was not clearly observed in the previous SST and gridded altimetry-derived map (Figure 2, b). In order to investigate the associated baroclinic

structure we now analyse the hydrographic fields from the glider measurements. This should provide insight about potential forcings related to the observed surface geostrophic flow.

4.1.3 Hydrography from glider measurements

Figure 4 shows the potential temperature (a), salinity (b) and density (c) profiles captured by glider for the northward transect, co-localized at surface with the altimetric track (results at southward transect, not shown here, are equivalent).

Figure 4

Concerning the potential temperature (Figure 4a), sub-mesoscale oscillations, less than 10 km in extent, can be observed in the first 50 m layer whereas below 50 m no marked signals appeared. Looking at the salinity profiles (Figure 4b), small-scale features (marked by relatively low salinity value of 38.0 - 38.1 psu) are also observed in the first 50 m of the water column. These structures are very different to the signals at greater depth (> 60 m) where marked horizontal salinity gradients appear. These (sub)surface salinity gradients are well phased with surface altimetric and glider current previously analysed: Table 3 shows that below 50 m the mean correlations between these salinity gradients and the across-track surface absolute geostrophic current are of 0.67 and 0.81 for respectively altimetry and glider (respectively -0.13 and 0.06 in the first 50 m). Since such significant (anti)correlations are not obtained with temperature gradients, this may indicate that local geostrophic currents are mainly driven by salinity and not temperature gradients.

Table 3

In order to quantitatively confirm or reject this assessment, two virtual density fields have been computed from two different ways (Figure 4 d, e) and compared to the density field derived from the “real” temperature (T) and salinity (S) profiles (“real”, Figure 4c). The first density field (Figure 4d) has been built by using the real potential temperature measurements but by considering, at each depth level, a constant salinity value (the horizontal spatial mean

391 from glider). In an opposite way, the second density field (Figure 4e) has been built by using
392 the real salinity field but by considering at each level depth a constant temperature value (the
393 spatial mean from glider). These imply that the first density field (“S fixed”, Figure 4d) does
394 not take into account effects due to the salinity gradients whereas the second one (“T fixed”,
395 Figure 4e) does not consider effects related to the temperature gradients. By comparing the
396 horizontal gradient of these 2 virtual density fields to the observed one (Figure 4c), it should
397 be therefore possible to evaluate the respective contributions of salinity and temperature to
398 the density gradient (and therefore on the across-track geostrophic flow).

399 The results are reported in Figure 4(f) which shows that for depth less than 50 m,
400 temperature gradients dominate since the percentage of std explained by the “S fixed” field in
401 the “real” density field is higher than 80% (close to 0% for “T fixed”). But below 50 m, the
402 percentage of std explained by the “S fixed” field progressively decreases whereas the
403 percentage of std explained by “T fixed” increase. Below 60 m depth the percentage of std
404 explained by “T fixed” field (> 70% below 100 m depth) is greater than for the “S fixed field”
405 (<20% below 100 m depth). This means that the contribution of the salinity gradients in the
406 density gradient computation becomes higher than the contribution of temperature gradient.
407 Therefore, the across track Geostrophic flow (proportional to the density gradient) associated
408 to the observed dynamical features seems mainly driven by sub-surface salinity gradients.

409 However, using only altimetry and glider data does not allow us to definitively conclude on
410 the origins of these strong salinity gradients. This would also require the complementary use
411 of modelling simulations. Thus, the next objective of this paper will be therefore to better
412 identify the origin and mechanisms associated to the observed small scale features. For this,
413 a regional model will also be used in conjunction with the previous multi-sensor observations.
414 However, it will be firstly necessary to check whether the model is able to realistically
415 reproduce the ocean dynamics at the Balearic Basin scale, both before and during the glider
416 mission. In second step, it would be also crucial to assess the models ability to adequately
417 simulate the observed patterns at the north of the Mallorca coast, specifically during the

glider mission. If so, we could confidently use it to explore the processes involved in the measurements from altimetry and gliders.

4.2 Model validation

4.2.1 Surface comparison with remote-sensing

4.2.1.1 Synoptic surface view for the July-August 2008 period

In this section, we proceed to first comparisons between the ROMS model outputs and remote-sensing data over the July-August 2008 period. In this respect, surface geostrophic current from altimetric gridded Absolute Dynamic Topography ((M)SLA+MDT) can be compared to the 2D model geostrophic currents derived from the model sea level height (interpolated on the same grid). Eddy Kinetic Energy (EKE) has been therefore calculated from these two consistent current fields and time-averaged over the period July-August 2008 (see Figure 5 b, d). To complement, we also computed, during the same period, the time-averaged SST from both simulation and satellite AVHRR data (see Figure 5 a,c). The temporal evolution of these two variables, spatially-averaged over the whole model domain, is also used in view of a quantitative comparison (Figure 6). The corresponding statistical results are reported in table 4.

Figure 5

Figure 6

Figure 5 shows a relative good general agreement between model and satellite data. Concerning SST (Figure 5,a,c), the Catalan front is clearly observed in the two SST fields, in the northern part of the model domain, separating relatively cold water (< 25°C) from warmer water (> 26 °C) located in the Balearic Sea. In the southern part of the domain, colder water patches observed in remote-sensing are also reproduced by the model. The time series of the spatial -averaged SST (Figure 6a) also show the model's ability to correctly simulate the SST variability observed by satellite measurements on the period July-August 2008. The

curves show a general SST decrease of 1°C between 01/07/08 and 20/07/08, an increase of 2.5°C between 21/07/08 and 06/08/08 and a decrease of 1°C until 31/08/08. Statistical results confirm this good agreement (see table 4): the model and satellite SST are characterized by the same mean temperature (26 °C), an absolute mean difference of 0.5 °C, a correlation higher than 0.9 and a close standard deviation (std) of 0.8°C and 1°C for respectively the model and the satellite observations.

Table 4

As expected, the agreement between the model and remote –sensing in terms of EKE is not as clear since the model is not constraint using data assimilation and, as noted previously, altimetric (M)SLA are not always adapted for regional studies. Relatively high mean EKE values (>500 cm^2/s^2) are observed in the two maps, especially at the south part of the domain but they are not co-localized (cf. Figure 5, b,d). The temporal evolution of the spatially-averaged EKE however shows very close tendencies with a general decrease of 20% between 01/07/08 and 06/08/08 followed by an equivalent increase between 06/08/08 and 27/08/08, exactly coincident with the SST decrease previously observed (see Figure 6 a,b). Statistics show a mean absolute difference between model and altimetry which represents 20% of the mean altimetric EKE (see table 4 and red curve on Figure 6,b). When the EKE anomaly is computed by removing the 2 month mean current both in model and altimetry (and therefore the impact of MDT in the altimetric currents), the results are quite different (see table 4, Figure not shown). In that case, the mean spatial EKE anomaly is of 66% and 80% less for respectively model and altimetry (refer to table 4 for the associated values), the STD become of the same order and the mean absolute difference is only of 18 cm^2/s^2.

These first assessments show that the model is able to adequately reproduce the general surface dynamics for the period July-August 2008, both for the spatial patterns and the associated temporal variability. In complement, we have also subdivided the model domain into 4 zones of equal surface (as shown in Figure 5) to discriminate the relative errors and

the contributions of each sub-region in terms of EKE and SST mean and variability. The obtained statistical results are reported in Appendix A and seems confirm the model is able to reproduce in a satisfactory way the surface ocean dynamics at the Balearic regional scale and for the period July-August 2008.

4.2.1.2 Surface changes during the glider mission

We now focus on two distinct periods of August 2008, in order to describe potential changes at the Balearic Basin scale just before (01/08/2008 to 12/08/2008) and during (from 13/08/2008 to 27/08/2008) the glider mission. These two periods correspond respectively to a relatively low and high EKE (Figure 6b) in addition a significant change in the trend of SST (Figure 6a) which tends at decreasing after 06/08/2008 (both observed and simulated).

As previously indicated, comparison between figure 2 and figure 7 confirms the good agreement between the ROMS simulation and remote-sensing data, specifically over the 2 periods in August 2008. The description of dynamical patterns is similar to that observed using remote sensing in section 4.1.1. In particular, the temperature appears cooler over the west part of the domain during the glider mission. Analysis of the model's atmospheric forcing (not shown) indicates this is likely due to a strong and cold wind event that increased local heat loss by turbulent heat fluxes and vertical mixing. The local SST cooling generates in turn a zonal temperature gradient that reinforces the northward geostrophic circulation and also leads to an increase of the mesoscale activity (as observed in the EKE, see the previous section and Appendix A)

Figure 7

A major difference between model and satellite observations however occurs near the Iberian coast and more generally in zone 3 (see Figure 2 and Figure 7) where a southward coastal current not reproduced by the model is observed. In addition to potential boundary condition issues, this disagreement may be due to standard altimetry limitations in the coastal zone (refer to introduction) as well as a lack of data required to constraint the MDT

computation (refer to Rio et al., 2007). Close to this area, a permanent and surely unrealistic cyclonic eddy centred at (1°E, 40.5°N) is also seen (present in the MDT and not in the (M)SLA). This structure, not reproduced by the ROMS simulation before and during the glider mission, is relatively far from the glider transect and altimetric track location (> 200 km) and should not have an impact on the following interpretations. Farther east, modelled and altimetric surface geostrophic circulation are quite similar (as it will be also confirmed in section 4.2.2) which confirms the previous statistics of EKE showing relative good results (except in zone 3, refer to Appendix A), when the damaging impact of the MDT is not removed. With regard to absolute geostrophic current, using a map of differences between two time periods allows us to precisely remove potential issues related to the MDT by dealing directly with the oceanic signal variability. Figure 8 shows that the changes during the glider of model and gridded altimetry spatial patterns are quite similar.

Figure 8

In particular both the model and satellite observations are marked by a reinforcement of the current intensity and of a negative vorticity associated with an anticyclonic eddy acceleration ("OBELIX", as noted previously in section 4.1.1). From Figure 8, it also turns out that BC intensity decreases by approximately 5 cm/s whereas the northward geostrophic current crossing the glider transect at north tends to increase. The middle part of the glider transect is characterized by low surface vorticity variability (and EKE, also see Figure 5 b, d) both in the model and gridded altimetry. However, weak geostrophic surface current signatures may hide more intense sub-surface Geostrophic currents (confirmed in the following section). Additionally, even if currents derived from altimetric map give a qualitative assessment of general geostrophic patterns at the Balearic Basin scale, the synoptic representation of the surface circulation at a sub-regional scale is compromised by the limitations due to the space/time smoothing effect from the optimal interpolation required to merge data from multiple altimeters (Dussurget et al., 2011).

4.2.2 Comparison with glider data

4.2.1.3 Hydrography

Figure 9

Figure 10

By comparing Figure 9 and Figure 4, it can be seen, at first sight, that the ROMS simulation and glider hydrographic profiles are in good agreement despite some differences (weak salinity gradient in the model) and spatial lags of about 10 km (BC more offshore in glider data). Moreover, the glider section show some wiggles in the first layer that may be due to internal wave heaving that are not reproduced by the model.

Concerning the potential temperature (Figure 9a), the model shows less spatial variability in the first 50 m layer where sub-mesoscale oscillations, less than 10 km in extent, were observed in glider profile. In this area, the temperature std is therefore 30 % less in the model and low correlations between model and glider are observed (Figure 10, top). Outside of the BC location (latitude > 40.2°N) and below 50 m depth, the temperature horizontal gradients are very weak (std < 0.5°C both in glider and model) implying correlations are not really significant. Despite this, glider and model show close general statistical profiles (std and mean, Figure 10, top) with depth-averaged mean temperatures of 15,8 °C and 16,1°C and std of 0.31°C and 0.25°C, respectively.

Concerning salinity, the mean model and glider profile are close and the correlations below 50 m are between 0.8 and 0.9 (Figure 10, middle). However even if the glider and model salinity profile are quite well phased, the sub-surface salinity std is twice stronger in glider than in model (see Figure 10). Indeed, as suggested by the salinity profile (see Figure 4b and Figure 9b), the sub-surface salinity gradients are stronger in glider than in the model. This could be at the source of an underestimation of model surface currents with respect to observations (as it will be noted in 4.2.2.2, also see Figure 2). As previously observed with glider measurements, these model salinity gradients are also well correlated with the surface

absolute Geostrophic current (correlations > 0.5, see Table 3 and Table 5) whereas it is not the case for temperature gradient.

Table 5

To precisely evaluate the relative contributions of salinity and temperature gradients to the model density gradient computation, the same experiment than for the glider has been performed. The results from model (Figure 6f) confirm that the sub-surface Geostrophic currents are also mainly driven by salinity gradients. Indeed, as in glider, the influence of model temperature gradients decreases for depth below 50 m. Moreover, Figure 6f also shows the impact of salinity gradients becomes higher than the impact of temperature gradients for depth higher than 100 m (whereas it was about 60 m depth in glider). This could explain why the correlations between the model and glider density profiles become significantly better below 100 m depth, where the salinity gradients dominate (correlation > 0.8, refer to figure 10, bottom).

Moreover, the water masses identified on Figure 4 (a,b) and Figure 9 (a,b) between 40.1°N and 40.4°N and between 40.6°N and 40.8°N, have the same hydrographic properties in both model and glider measurements (low salinity less than 38.1 psu and temperature of 14°C at 70 m) which suggest they have the same origin but have followed two different trajectories. This is consistent with the 2D surface analysis done in 4.1.2 (also confirmed in 4.2.1.2 with model outputs) where the OBELIX eddy was shown to partially feed the BC at south whereas its northern part interacted with the NC return loop and advected water northward. The origin of this water mass, characterized by lower salinity value at the source of local salinity gradients (and therefore geostrophic flows), will be discussed in section 4.3.

4.2.1.4 Currents

The model surface relative geostrophic current has been computed with respect to the 180 m reference depth (as in glider) and has been interpolated to the glider track in space and time. Figure 11 shows comparisons with the ones obtained from glider hydographic measurements

578 at northward (13/08/08 - 20/08/08, Figure 11a), and southward transect (21/08/08 –
579 27/08/08, Figure 11b).

580 **Figure 11**

581 **Table 6**

582 Despite spatial lags of a few kilometers, Figure 11 shows that the modelled and glider
583 relative surface geostrophic current are consistent, with a mean difference less than 1 cm/s
584 and correlations respectively of 0.91 and 0.52 for northward and southward transect (see
585 table 6 for statistics). For the northward glider transect (Figure 5, a), model and glider show a
586 decrease of the current intensity from 5 cm/s to 0 cm/s in the cross-shore direction, at the BC
587 mean location (40.1 °N-40.5 °N). For the southward transect (Figure 5, b) the situation
588 becomes different with a BC relative surface geostrophic current larger, but twice less
589 intense. Northern BC, the relative geostrophic current is alternatively negative (southward)
590 and positive (northward) with a current intensity of +/- 5 cm at northward and southward
591 transect for both glider and model.

592 The comparisons between the absolute surface geostrophic currents from model and
593 observations show a relatively good agreement at the northward transect (significant
594 correlations of 0.78 and 0.50 with respect to glider and along-track altimetry), which is not the
595 case of the southward transect marked by a 20 km spatial lag (see Figure 3). Moreover, the
596 amplitude of absolute currents (both Geostrophic and total) from model is much less than in
597 the observations despite the good agreement previously observed in terms of surface
598 relative geostrophic currents. Therefore, this should also correspond to an underestimation of
599 sub-surface currents in the model.

600 From the analysis in 4.1.3, it followed that the surface altimetric and glider absolute
601 geostrophic current - an “integrated value” – reflected the salinity gradients signals of depth
602 and not the surface layer where small spatial scale disturbances hide a more stable deep
603 geostrophic signals. Therefore, we investigate and compare the patterns in distribution of
604 currents along the water column, both from model and from glider measurements (Figure 12)

Figure 12

When the absolute geostrophic current (Figure 12 b,d) and the relative Geostrophic current (Figure 12 a, c) are compared it can be logically seen that the features are quite different both in terms of magnitude and spatial distribution. In both cases the BC is however located between 40.1 °N and 40.3°N with a maximum intensity at 50 m depth, but the absolute current intensity is three times larger than the relative geostrophic current (10-20 cm/s as compared to 5-8 cm/s). The BC observed by the gliders was wider (up to 40.4°N) and stronger than the current simulated by the model. Between the BC and NC return-branch, a sub-surface feature is observed by the glider and partially reproduced by the model (see red square on Figure 12 b, d). Although the model structure shows a spatial lag of approximately 10 km towards the south, it shows alternatively a positive (northward) and negative (southward) current with maximum intensity at depths higher than 50 m for the positive current values in the model and the negative ones in glider (at latitude 40.6 °N).

The next challenge will be, by the use of the validated model, to describe the characteristics and the potential processes associated with this structure, intercepted north of Mallorca (previously called “ASTERIX” in 4.1.2).

4.3 Spatio-temporal variability from numerical modelling

Three virtual boxes are located at critical places chosen with respect to the previous analyses done with the multi-sensor data and oceanic model outputs: The first box (red box in Figure 7, b) is aimed at monitoring the time variability of hydrological and dynamical properties of the south water entering through the Ibiza Strait. The two other boxes are located at each side of the glider transect in order to assess the hydrological and dynamical changes both close to the ASTERIX site (black box in Figure 7, b) and in the vicinity of the NC retroflection (blue box in Figure 7, b).

Figure 13 shows the T/S diagrams, as a function of depth and horizontally space-averaged, at the three locations during the July-August 2008 period. It clearly demonstrates that water

in the south (Box 1) shows hydrographical properties very different to that of the water to the north (Box 2 and Box 3). Indeed, the water-mass here seems mainly constituted by recently modified AW characterized by a salinity of about 0.5 less than the 'older' more modified AW of northern origin (see section 2). Moreover, the T/S diagram in Box 1 (recent AW) is more dispersed than that of Boxes 2 and 3 (older AW), which suggests a progressive change of water masses properties during the 2 month study period.

Figure 13

In order to quantitatively assess the temporal evolution of the water masses' characteristics in the three boxes and their potential interaction, we now use a Hovmöller diagram of horizontal space-averaged key variables: salinity, current magnitude and relative vorticity, as a function of time and depth (see Figure 14).

Figure 14

Figure 14 shows that the salinity anomaly (removing the 2 month mean value) in the Ibiza Strait becomes significantly negative from mid-July to mid August. This strong decrease in the salinity anomaly coincides with an increase of the total current at depth (5 cm/s at 50 m depth). This corresponds to an entrance of less salty AW that is progressively modified and advected northward by the general circulation until it reaches the OBELIX location in August 2008. At the north-west side of the glider transect (Box 2), the situation of July shows a strong current magnitude (+15 cm/s) and alternating relative vorticity (+/- 2.10^{-5} /s). This corresponded to the cyclonic NC position that moved southward or northward in function of its interaction with southern currents (as also observed on Figure 16). In August 2008, a positive salinity anomaly of 0.05 - 0.1 is observed, associated with a decrease of current intensity. This corresponds to the period OBELIX progressively expands to the north and interacts with the NC return loop. Consequently the less salty AW entering through the Ibiza Strait is advected northward until it reaches salty water from the NC system, at the time of the glider mission (see dashed line on Figure 14). Indeed, Figure 14 (Box 3) show a negative salinity anomaly of 0.1 psu in August 2008, associated with a relatively strong deep current

(approx. 5cm/s at surface and 10 - 15 cm/s from 30 m to 200 m). At the same time, a negative sub-surface relative vorticity is generated at depth, in the neighbourhood of the glider transect, with maximum values of -3 x 10^{-5}/s. This relatively strong negative vorticity is time-correlated (>0.9, see Figure 15) with the sub-surface salinity difference observed between Box 2 and Box 3 (~0.2 PSU over a few km). We will now try to identify the 2D horizontal structure associated with this sub-surface negative vorticity signature, generated close to Box 3, in the neighbourhood of the glider transect.

Figure 15

Figure 16 shows the relative vorticity temporal evolution (from July 2008 to August 2008) in order to characterize the 2D horizontal shear of the velocity field. For this, the model relative vorticity has been computed at 2 depth levels in order to also take into account the baroclinic structure of features previously observed.

Figure 16

From figure 16 it follows that a subsurface mesoscale anticyclonic structure is generated in the North-east of the model domain, at time of the glider mission, in close vicinity to the transect and a ROMS boundary (there are no continuity issues with respect to MFS as noted in section 3.3). View the relative good agreement previously established between model and observations (both qualitatively and quantitatively), our major but realistic hypothesis is that the same kind of structure has been intercepted by the glider and along-track altimetry measurements. Given its small scale extension (<30 km) and its relative weak signature in surface, this structure was not clearly observed with gridded altimetry product. However, it is remarkable to note that both the model relative vorticicity and associated currents of ASTERIX are significantly stronger at 75 m depth than at 10 m which is in line with the previous sub-surface glider observations done in its neighbourhood, north of Mallorca. The intensity of the ASTERIX eddy appears to be controlled by a salinity gradient (as the structure observed by the glider profiles), created by the meeting of two distinct, energetic water flows. The first water flow is mainly constituted of recent AW entering through the Ibiza

686 Strait, which is then progressively modified and advected by the general circulation until it
687 reaches the ASTERIX area at time of the glider mission. This small-scale anticyclonic eddy,
688 whose residual currents, at south, has been partially captured by the glider transect and
689 along-track PISTACH data, seems therefore due to baroclinic interaction between this water
690 mass and saltier Mediterranean waters (old AW) coming from the NC cyclonic circulation
691 located to the north.

692

693 # 5. Discussion and conclusions

694 In this study, the potential synergies between the multi-source remote-sensing, glider and
695 numerical model have been discussed in terms of accuracy, resolution and spatial/temporal
696 sampling. New methodologies have been tested in order to improve the consistency between
697 altimetry and glider datasets, by using experimental altimetry data from PISTACH project
698 (Coastal and Hydrology Altimetry product handbook, 2010) and by computing glider absolute
699 geostrophic currents following the recent strategy described in Bouffard et al. (2010). The
700 oceanic model and multi-sensor dataset were then used in conjunction in order to interpret
701 the observed physical processes. By increasing the confidence in the dynamical structure
702 interpretation, this approach has led to a full characterization of small-scale processes. We
703 believe that the worldwide challenge of coastal (sub)mesoscale dynamics characterization
704 have to be addressed locally through such an integrated approach combining both
705 observations and free numerical runs. This is especially true in an area where small
706 mesoscale structures are characterized by low signal to noise ratio, indeed associated
707 surface signatures are particularly weak in the north western Mediterreanean and therefore
708 difficult to interpret with the single use of isolated measurements.

709 Even if the obtained results are quite encouraging, our comparisons have also shown the
710 limitations of these two observation systems, both in terms coverage and accuracy. Focused
711 on the glider platform, the observed bias at time of back transect could be further reduced
712 through applying additional corrections to the glider depth averaged GPS currents. In

particular, we would expect to achieve better results with a more accurate estimation of the error in the glider displacement assumptions which imply a more accurate measurement of glider heading. With regards to the gridded altimetric product and the MDT used, we have also confirmed the relative poor resolution of existing products that should require both a better satellite constellation coverage in addition to a regional approach in order to better constraint the representatively of local mesoscale features (refer to Dussurget et al., 2011). Furthermore, experiments based on glider versus along-track altimetry cross comparisons need to be repeated in order to improve and consistently assess the impact of new methods dedicated to coastal zone applications. Indeed, the promising early results in coastal altimetry (refer to Vignudelli et al., 2011 for a review) support the need for continued research and scientific applications, with the opportunity of providing inputs and recommendation to future satellite missions (refer to the SWOT satellite and last Coastal Altimetry Workshop, San Diego 2011).

In this study, in addition to multi-sensor cross comparisons, particular attention has been paid to the model validation and the characterization of a small-scale (<30 km) anticyclonic eddy observed by glider, along-track altimetry and partially reproduced by a ROMS simulation, north of Mallorca. The subsurface salinity gradient associated to this structure seems to result from a recent Atlantic Water inflow through the Ibiza Channel that is advected northward and interacts with saltier old Atlantic Water flowing with the Northern Current. It has been shown the local geostrophic currents during the glider mission were mainly driven by these salinity gradients and not, as usual in the Balearic Sea, by temperature gradients, which represent a major finding with respect to previous studies over this area (e.g. Pascual et al. 2002; Pinot et al. 2002; Rubio et al., 2009).

This study therefore demonstrates the key role of water mass exchanges and particularly salinity properties between the northern Gulf of Lions and the southern Algerian Basin through the Balearic Island channels. The Ibiza and Mallorca channels provide a significant passage for water masses potentially interacting with the northern general circulation, which

emphasizes the importance of monitoring the entrance of recent Atlantic Water as an indicator of the mesoscale climatology in the north western Mediterranean Sea.

ACKNOWLEDGEMENTS

We deeply acknowledge the contribution of M. Martínez-Ledesma and B. Casas during the data acquisition phase of the glider missions. Special thanks are also due to B. Buongiorno Nardelli, R. Escudier , A. Petrenko and A. Doglioli for fruitful discussions concerning the interpretations of data and simulations. The authors are also grateful to B. Garau for processing glider data and to E. Heslop and R. Campbell for high valuable editing comments as well as to G. Vizoso for ROMS numerical setup and data management. The altimeter (M)SLA were produced by SSALTO/DUACS and distributed by AVISO with support from CNES. The coastal high-resolution altimeter products were produced by CLS and distributed by AVISO within the PISTACH project supported by CNES. Sea surface temperature images were acquired and processed by EUMETSAT. This work was supported by the European Commision MyOcean Project (SPA.2007.1.1.01— development of upgrade capabilities for existing GMES fast-track services and related operational services; Grant Agreement 218812-1-FP7-SPACE 2007-1).

APPENDIX

(A) Complementary validation of the model

The assessments done in section 4.2 show the model's ability to reproduce adequately the general surface dynamics for the period July-August 2008 (both for the spatial patterns and the associated temporal variability). Here, we subdivide the model domain into 4 zones of equal surface (as shown in Figure 5) to discriminate the relative errors and the contributions of each geographic area in terms of EKE and SST mean and variability: Zone 1 and Zone 2 mainly aim at monitoring dynamical characteristics related to northward flows potentially entering through the Ibiza and Mallorca channels. Zone 3 and Zone 4 are chosen to characterize the temporal evolution of frontal dynamics occurring north of Mallorca, in the neighbourhood of the glider transect located at the interface between the Balearic front and the CN return loop (ref to Figure 1).

Concerning the SST temporal evolution (see Figure A1), the comparison shows results similar to those obtained over the whole domain (absolute difference < 0.5 °C, see table A1). The major SST variations observed both by satellite and numerical simulations occur from 06/08/08 to 27/08/08, during the glider mission. At this time, Figure A1 shows a relatively strong SST decrease (greater than 1.5°C in zone 1 and zone 3 ,less than 1°C in zone 2 and zone 4), which correspond respectively to the west and the north-West part of the model domain.

Figure A1

Table A1

Concerning the absolute EKE, significant differences are observed in function of the considering zone. Except for zone 3, table A2 shows the mean absolute difference is less than 23% of the mean differences between model and altimetry (also refer to red curves on figure A2). This shows the relatively good coherence between the two geostrophic current fields. The more energetic area is zone 2 with a mean model (respectively altimetric) EKE of

230 cm^2/s^2 (respectively 270 cm^2/s^2) and a standard deviation of 65 cm^2/s^2 (respectively 44 cm^2/s^2). Except for zone 4 in altimetry, a significant increase of the EKE (between 25 % and 50%) is observed from 06/08/2008 to 27/08/2008, while a general SST decrease is simultaneously observed and simulated. When considering zone 3, it appears that the observed discrepancies between the model and observations seems mainly due to the MDT used for the altimetric absolute geostrophic current computation. Indeed when EKE is computed by removing the 2 month mean current (and therefore the impact of MDT in altimetry), the agreement between model and altimetry EKE anomaly is strongly improved with a mean absolute difference of 30 % of the mean EKE anomaly (see Table A2). This implies that, over this area, the current variability is consistent despite significant differences in terms of mean geostrophic current.

Figure A2

Table A2

Figure captions:

Figure - 1 (a): Bathymetry of the Western Mediterranean Sea with ROMS and WRF domains (in red and black respectively). (b): zoom of the ROMS domain, glider northward transect (southward transect is equivalent) and J2 altimetric track 70 (yellow) overlapped by the main permanent currents (white arrows) and typical mesoscale events (dashed white arrow). NC means Northern Current, BC means Balearic Current and AW means Atlantic Water.

Figure 2 - Time-averaged SST (AVHRR) overlapped by the gridded altimetric geostrophic current (a) before (01/08/2008 to 12/08/2008) and (b) during (13/08/2008 to 27/08/2008) the glider mission.

Figure 3 - Comparisons of absolute surface currents (in cm/s) interpolated at the glider location at northward (a) and southward (b) transect (Large curves correspond to 15km-smoothed

signals). The blue curve corresponds to the glider rebuilt across-track absolute surface geostrophic current (by using a reference level correction as described in section 3.2). The red curve corresponds to the instantaneous altimetric across-track absolute surface geostrophic current derived from along-track PISTACH data (+MDT, (a): cycle 4 of JASON2; (b): cycle 5 of JASON2). The grey curve corresponds to the space/time interpolated altimetric across-track absolute surface geostrophic current derived from AVISO ((M)SLA +MDT). The large black curve corresponds to the space/time interpolated model across-track absolute surface geostrophic current and the thin curve to the model across-track total surface current. BC, NC and the associated separations symbolise respectively the supposed mean position of the Balearic Current and of a retroflection branch of the Northern Current.

Figure 4 - Potential temperature (a), salinity (b) and density (c) glider profiles at northward transect (equivalent result for southward transect), as a function of depth (m) and latitude (°N). (d) Potential density computed by removing the salinity gradients. (e) Potential density computed by removing the temperature gradients. The white dashed line on (a), (b), (c), (d) and (e) correspond to 60m depth. (f) Black curve: Percentage of std explained by (d) in (c) as a function of depth (in m). Blue curve: Percentage of std explained by (e) in (c) as a function of depth (in m)

Figure 5 - Time-averaged Sea Surface Temperature in °C and Eddy Kinetic Energy (EKE) in cm^2/s^2 for the period July-August 2008 from model (c,d) and remote sensing, derived from altimetry (AVISO (M)SLA+MDT) for EKE (b) and satellite AVHRR for SST (a).

Figure 6 - Time series of spatially-averaged (over the model domain) SST and EKE derived from model and satellite (AVHRR and AVISO (M)SLA+MDT). The red curve corresponds to the absolute difference between model and satellite EKE

Figure 7 - Time-averaged SST overlapped by the geostrophic current (a) before (01/08/2008 to 12/08/2008, top) and (b) during (13/08/2008 to 27/08/2008, bottom) the glider mission from the

ROMS oceanic model. Boxes used to monitor the water mass characteristics (in Figure 13 and 14 and 15) have also been added.

Figure 8 - Temporal difference of surface geostrophic current (vectors) and relative vorticity before (01/08/2008 to 12/08/2008) and during (13/08/2008 to 27/08/2008) the glider mission from ROMS model (b) and altimetric data from AVISO (M)SLA+MDT (a) in the close vicinity of the glider transect (line red for the northward transect)

Figure 9 – Potential temperature (a), salinity (b) and density (c) model profiles space time interpolated at the northward glider transect (equivalent result for southward transect), as a function of depth (m) and latitude (°N). (d) Potential density computed by removing the salinity gradients. (e) Potential density computed by removing the temperature gradients. The white dashed line on (a), (b), (c), (d) and (e) correspond to 60m depth. (f) Black curve: Percentage of std explained by (d) in (c) as a function of depth (in m). Blue curve: Percentage of std explained by (e) in (c) as a function of depth (in m)

Figure 10 – Statistical comparisons between model and glider hydrographic measurements (potential temperature, salinity and density) as a function of depth (m). Blue curves correspond to statistics from glider (both STD and mean), black curves correspond to statistics from model. The red curve corresponds to the correlation between model and glider measurements.

Figure 11 - Comparisons between glider (blue curves, raw and 15 km smoothed data) and space/time interpolated model (black curve) relative across-track surface Geostrophic current as a function of latitude (reference level at 180 m) at time of (a) northward (13/08/2008 to 20/08/2008) and (b) southward transect (right, 21/08/2008 to 27/08/2008)

Figure 12 – Comparisons between glider and ROMS across-track currents (cm/s) as a function of latitude (°N), through the water column (0-180 m). Relative geostrophic current derived from

the DH calculated with respect to 180 m depth from the ROMS model (a) and from glider measurements (c) Rebuilt absolute geostrophic current by using the methodology described in section 2.2 from ROMS (b) and glider measurements (d). The BC and a sub-surface mesoscale structure are respectively highlighted by a black square and a red square.

Figure 13 - T/S diagram from the model (in °C and PSU) in function of depth (m) from July 2008 to August 2008, spatially-averaged (but not time averaged) for each of the 3 boxes (refer to Figure 15, for the location of the boxes)

Figure 14 - Model spatially averaged salinity anomaly (a), total absolute current norm (b) and relative vorticity (c) as a function of time and depth in the three boxes. Top: Ibiza Channel neighbourhood (Box 1), middle: NC retroflection neighbourhood (Box 2), bottom: glider Westside neighbourhood (Box 3). The dashed lines correspond to the glider mission period.

Figure 15 - Time series of the model salinity difference (PSU) between Box 2 and Box 3 (green curve right axis) and of the model relative vorticity ($10^{-5}.s^{-1}$) in box 3, at the ASTERIX location. The dashed lines correspond to the glider mission period.

Figure 16 - Relative vorticity ($10^{-5}.s^{-1}$) in the ROMS model from the beginning of July to the end of August 2008 at (a) 10 m depth and (b) 75 m depth. (a) boxes used to monitor the water mass characteristics in Figure 13 and 14 and 15. (b) The blue and black circles highlight the relative vorticity signatures associated respectively to the large scale (OBELIX) and small scale (ASTERIX) anticyclonic eddies

Figure A1 - Time series of spatially-averaged (over the 4 subdivided domains, ref to Figure 5) SST from model and AVHRR satellite data.

Figure A2 - Time series of spatially-averaged (over the 4 subdivided domains, ref to Figure 5) EKE associated to geostrophic currents derived from model and satellite altimetry (AVISO (M)SLA +MDT). The red curve corresponds to the absolute difference between model and satellite EKE.

REFERENCES

Alvarez, A, Tintoré, J., Sabatés, A., 1996. Flow modification and shelf-slope exchange induced by a submarine canyon off the northeast Spanish coast. J Geophys Res 101: 12043–12055.

Anzenhofer, M., Shum, C.K., Rentsh, M., 1999. Coastal altimetry and applications, Tech. Rep. No 464, Geodetic Science and Surveying, The Ohio State University Columbus, USA.

Astraldi, M., Balopoulos, S., Candela, J., Font, J., Gacic, M., Gasparini, G.P., Manca, B., Theocharis, A., Tintore´, J., 1999. The role of straits and channels in understanding the characteristics of Mediterranean circulation, Prog., Oceanogr.,44, 65– 108

Birol F., Cancet, M., Estournel, C., 2010. Aspects of the seasonal variability of the Northern Current (NW Mediterranean Sea) observed by altimetry, Journal of Marine Systems, 81, pp 297-311, doi:10.1016/j.jmarsys.2010.01.005.

Bouffard J., Roblou, L., Birol, F., Pascual, A., Fenoglio-Marc, L., Cancet, M., Morrow, R., Ménard, Y., 2011. Introduction and assessment of improved coastal altimetry strategies: case study over the North Western Mediterranean Sea, in S. Vignudelli, A.G. Kostianoy, P. Cipollini, J. Benveniste (eds.), *Coastal Altimetry,* Springer-Verlag Berlin Heidelberg, 2011. DOI: 10.1007/978-3-642-12796-0_12

Bouffard, J., Pascual, A., Ruiz, S., Faugère, Y., Tintoré, J., 2010. Coastal and mesoscale dynamics characterization using altimetry and gliders: A case study in the Balearic Sea, J. Geophys. Res., 115, C10029, doi:10.1029/2009JC006087.

Bouffard, J., Vignudelli, S., Cipollini, P., Menard, Y., 2008. Exploiting the potential of an improved multimission altimetric data set over the coastal ocean, Geophys. Res. Lett., 35, L10601, doi:10.1029/2008GL033488.

Capet, X, , P. Klein, B. L. Hua, G. Lapeyre, et J. C. McWilliams, 2008c. Surface kinetic and potential energy transfer in SQG dynamics. *J. Fluid Mech*., 604, 165–174.

Capet, X., J. C. McWilliams, M.J. Molemaker and A.F. Shchepetkin, 2008b. Mesoscale to Sub mesoscale transition in the California Current System. Part 2. Dynamical Processes and Observational Tests, *J. Phys. Oceanogr.*, 38, 44-64.

Capet, X., J. C. McWilliams, M.J. Molemaker, et A.F. Shchepetkin, 2008a : “Mesoscale to submesoscale transition in the California current system. Part I : Flow structure, eddy flux, and observational tests.” *J. Phys. Oceanogr.*, 38, 29–43.

Coastal and Hydrology Altimetry product (PISTACH) handbook, *SALP-MU-P-OP-16031-CN 01/00,* edition 1.0, October 2010.

Chelton, D. B., M. G. Schlax, and R. M Samelson, 2011: Global observations of nonlinear mesoscale eddies. *Prog. Oceanogr.*, 91, 167-216.

Ducet, N., Le Traon, P.Y., Reverdin, G., 2000. Global high-resolution mapping of ocean circulation from TOPEX/Poseidon and ERS-1 and-2. J. Geophys. Res.-Oceans, 105:19477-19498.

Dussurget R., F Birol, R.A. Morrow, et P. De Mey (2011). Fine Resolution Altimetry Data for a Regional Application in the Bay of Biscay. Marine Geodesy 2, n°. 34: 1-30

Emery, W.J., T. Strub, R. Leben, M. Foreman, J.C. McWilliams, G. Han, C. Ladd, and H. Ueno, 2011. Satellite Altimetry Applications off the Coasts of North America, in S. Vignudelli, A.G. Kostianoy, P. Cipollini, J. Benveniste (eds.), *Coastal Altimetry,* Springer-Verlag Berlin Heidelberg, 2011. DOI: 10.1007/978-3-642-12796-0_16

945 Fairall, C. F., E. F. Bradley, J. E. Hare, A. A. Grachev, and J. B. Edson, 2003. Bulk
946 parameterization of air-sea fluxes: Updates and verification for the COARE algorithm, J.
947 Clim., 16, 571 – 591

948 Font, J., 1990. A comparison of seasonal winds with currents on the continental slope of the
949 Catalan Sea (Northwestern Mediterranean) J. Geophys. Res., 95 (C2): 1537-1546.

950 Font, J., Salat, J., Tintoré, J., 1988. Permanent features of the circulation in the Catalan Sea.
951 Oceanologica Acta, 51-57.

952 Fu, L.L., Chelton, D.B., Le Traon, .Y. and R. Morrow, 2010a. Eddy dynamics from Satellite
953 altimetry. .Oceanography, Volume 23, Number 4, a quarterly journal of The
954 Oceanography Society.

955 Fu, L-L., Alsdorf, D., Rodriguez, E., Morrow, R., Mognard, N., Lambin, J., Vaze, P. & Lafon,
956 T., 2010b. “The SWOT (Surface Water and Ocean Topography) Mission: Spaceborne
957 Radar Interferometry for Oceanographic and Hydrological Applications”, in Proceedings
958 of the "OceanObs’09: Sustained Ocean Observations and Information for Society"
959 Conference (Vol. 2), Venice, Italy, 21-25 September 2009, Hall, J., Harrison D.E. and
960 Stammer, D., Eds., ESA Publication WPP-306, 2010.

961 Garau, B, S Ruiz, W G. Zhang, A Pascual, E Heslop, J Kerfoot and Joaquín Tintoré, 2011:
962 Thermal Lag Correction on Slocum CTD Glider Data. *J. Atmos. Oceanic Technol.*, 28,
963 1065–1071. doi: http://dx.doi.org/10.1175/JTECH-D-10-05030.1

964 Garreau, P, V. Garnier, A. Schaeffer, 2011: Eddy resolving modelling of the Gulf of Lions and
965 Catalan Sea, Ocean Dyn., 61 (7) (2011), pp. 991–1003

966 Ginzburg, A.I., A.G. Kostianoy, N.A. Sheremet, and S.A. Lebedev, 2011. Satellite Altimetry
967 Applications in the Black Sea , in S. Vignudelli, A.G. Kostianoy, P. Cipollini, J. Benveniste
968 (eds.), *Coastal Altimetry,* Springer-Verlag Berlin Heidelberg, 2011. DOI: 10.1007/978-3-
969 642-12796-0_14

970 Gourdeau, L., Kessler, W.S., Davis, R.E., Sherman, J., Maes, C., Kestenare, E., 2008. Zonal
971 Jets Entering the Coral Sea, J. Phys. Oceanogr., Vol. 38, 715-725, doi:
972 10.1175/2007JPO3780.1.

973 Haidvogel, D. B., Arango, H., Hestrom, K., Beckmann, A., Malanotte- Rizzoli, P.,
974 Shchepetkin, A., 2000. Model evaluation experiments in the North Atlantic basin:
975 Simulations in nonlinear terrain-following coordinates, Dyn. Atmos. Oceans, 32, 239–
976 381.

977 Hátún, H., Eriksen, C.C., Rhines, P.B., 2007. Buoyant Eddies Entering the Labrador Sea
978 Observed with Gliders and Altimetry. J. Phys. Oceanogr., 37, 2838-2854.

979 Hodges, B.A. and Fratantoni, D.M., 2009. A thin layer of phytoplankton observed in the
980 Philippine Sea with a synthetic moored array of autonomous gliders, J. Geophys. Res.
981 114, C10020, doi:10.1029/2009JC005317.

982 Hu, Z.H., Doglioli A., Petrenko A., Marsaleix P., Dekeyser I., 2009. Numerical Simulation of
983 mesoscale eddies in the Gulf of Lion, *Ocean Modelling*, Vol. 28/4, pp. 203-208, doi :
984 10.1016/j.ocemod.2009.02.004.

985 Hu, Z.Y., Petrenko, A.A., Doglioli, A.M., Dekeyser, I., 2011. Study of coastal eddies:
986 application in the Gulf of Lion. *J. Marine Syst.*,Volume 88, Issue 1, Pages 3-11.

987 Kouraev, A.V., J.-F. Crétaux, S.A. Lebedev, A.G. Kostianoy, A.I. Ginzburg, N.A. Sheremet,
988 R. Mamedov, E.A. Zakharova, L. Roblou, F. Lyard, S. Calmant, and M. Bergé-Nguyen,
989 2011. Satellite Altimetry Applications in the Caspian Sea. in S. Vignudelli, A.G. Kostianoy,
990 P. Cipollini, J. Benveniste (eds.), *Coastal Altimetry,* Springer-Verlag Berlin Heidelberg,
991 2011. DOI: 10.1007/978-3-642-12796-0_15

992 Klein, P. and G. Lapeyre, 2009. The oceanic vertical pump induced by mesoscale and
993 submesoscale turbulence. *Annual Review of Marine Science* 1:351–375.

994 La Violette, P. E., Tintoré, J., Font, J. 1990: The surface circulation of the Balearic Sea. J.
995 Geophys. Res., 95, 1559-1568.

996 Le Traon, P.-Y., and Morrow, R., 2001. Ocean currents and mesoscale eddies, in Satellite
997 Altimetry and Earth Sciences: A Handbook of Techniques and Applications, edited by L.-
998 L. Fu and A. Cazenave, pp. 171– 215, Academic, New York.

999 Lebedev, S.A., A.G. Kostianoy, A.I. Ginzburg, D.P. Medvedev, N.A. Sheremet, and S.N.
1000 Shauro, 2011. Satellite Altimetry Applications in the Barents and White Seas in S.
1001 Vignudelli, A.G. Kostianoy, P. Cipollini, J. Benveniste (eds.), *Coastal Altimetry,* Springer-
1002 Verlag Berlin Heidelberg, 2011. DOI: 10.1007/978-3-642-12796-0_15

1003 Lehahn, Y., d'Ovidio, F., Levy, M. & Heifetz, E. Stirring of the Northeast Atlantic spring bloom:
1004 a Lagrangian analysis based on multisatellite data. *J. Geophys. Res.* 112, C08005
1005 (2007).

1006 Lévy, M., 2008. The modulation of biological production by oceanic mesoscale turbulence. In
1007 Transport in Geophysical Flow: Ten Years After, ed. JBWeiss, A Provenzale, vol. 744 of
1008 Lect. Notes Phys. Berlin: Springer, pp. 219–61.

1009 Marchesiello, P., McWilliams, J., Shchepetkin, A., 2001. Open boundary conditions for
1010 longterm integration of regional oceanic models. Ocean Modelling, 3(1):20.

1011 Martin, J. P., Lee, C. M., Eriksen, C., Ladd, C., Kachel, N. B., 2009a. Glider observations of
1012 kinematics in a Gulf of Alaska eddy, J. Geophys. Res., 114, C12021,
1013 doi:10.1029/2008JC005231.

1014 Martin, J., Lee, C., Eriksen, C., Ladd, C., Kachel, N., 2009b. A two-month seaglider survey of
1015 a gulf of alaska eddy: How dynamical structure evolves temporally. ser. Eos Transactions
1016 AGU, vol. 52, no. 87, Fall Meeting 2006, abstract OS34A-02.

1017 McGillicuddy, D.J. Jr., Robinson, A.R., Siegel, D.A., Jannasch, H.W., Johnson, R., Dickey,
1018 T.D., McNeil, J., Michaels, A.F., Knap, A.H., 1998. Influence of mesoscale eddies on new
1019 production in the Sargasso Sea. Nature 394, 263–265.

Merckelbach, L.M., Briggs, R.D., Smeed, D.A., Griffiths, G., 2008. Current measurements from autonomous underwater gliders, 9th Working Conference on Current Measurement Technology. Ieee, Charleston, SC, pp. 61-67.

Morrow, R. and Le Traon, P.-Y. 2011: Recent advances in observing mesoscale ocean dynamics with satellite altimetry. J. Adv. Space Res., doi:10.1016/j.asr.2011.09.03

Nencioli, F., F. d'Ovidio, A. M. Doglioli, and A. A. Petrenko, 2011. Surface coastal circulation patterns by in-situ detection of Lagrangian coherent structures, *Geophys. Res. Lett.*, 38, L17604, doi:10.1029/2011GL048815.

Niewiadomska, K., Claustre, H., Prieur, L., D'Ortenzio, F., 2008. Submesoscale physical-biogeochemical coupling across the Ligurian current (northwestern Mediterranean) using a bio-optical glider, Limnology and Oceanography, 53, 2210-2225.

Pascual, A., Buongiorno Nardelli, B., Larnicol, G., Emelianov, M., Gomis, D., 2002. A case of an intense anticyclonic eddy in the Balearic Sea (western Mediterranean), J. Geophys. Res., 107(C11), 3183, doi:10.1029/2001JC000913.

Pascual, A., Gomis, D., Haney, R.L. Ruiz, S., 2004. A quasigeostrophic analysis of a meander in the Palamós canyon: vertical velocity, geopotential tendency and a relocation technique, Journal of Physical Oceanography, 34, 2274-2287.

Pascual, A., M. I. Pujol, G. Larnicol, P. Y. Le Traon, and M. H. Rio (2007), Mesoscale mapping capabilities of multisatellite altimeter missions: First results with real data in the Mediterranean Sea, Journal of Marine Systems, 65(1-4), 190-211.

Pascual, A., S. Ruiz, and J. Tintoré (2010), Combining new and conventional sensors to study the Balearic Current, Sea Technology, 51(7), 32-36.

Pascual, A., Y. Faugère, G. Larnicol, and P.-Y. Le Traon (2006), Improved description of the ocean mesoscale variability by combining four satellite altimeters, Geophys. Res. Lett., 33, L02611, doi:10.1029/2005GL024633.

1045 Perry, M. J., B. S. Sackmann C. C. Eriksen, and C. M. Lee. 2008. Seaglider observations of
1046 blooms and subsurface chlorophyll maxima off the Washington coast. Limnol. Oceanogr.
1047 53: 2169–2179.

1048 Pinardi, N., Allen, I., De Mey, P., Korres, G, Lascaratos, A, Le Traon, P.Y., Maillard, C.,
1049 Manzella, G., Tziavos, C., 2003. The Mediterranean Ocean Forecasting System: first
1050 phase of implementation (1998-2001). Ann. Geophys., 21, 1, 3-20.

1051 Pinot, J.M., López-Jurado, J.L., Riera, M., 2002. The CANALES experiment (1996-98).
1052 Interannual, seasonal, and mesoscale variability of the circulation in the Balearic
1053 Channels. Prog. Oceanog., 55, 335-370.

1054 Pinot, J.M., Tintore´, J., Gomis, D., 1995. Multivariate analysis of the surface circulation in the
1055 Balearic Sea, Prog. Oceanogr., 36, 343–376.

1056 Powell, B. S., and R. R. Leben, 2004. An optimal filter for geostrophic mesoscale currents
1057 from along-track satellite altimetry, J. Oceanic and Atmos. Tech., 21:16331642.

1058 Rio, M. H., Poulain, P. M., Pascual, A., Mauri, E., Larnicol, G., Santoleri, R., 2007. A mean
1059 dynamic topography of the Mediterranean Sea computed from altimetric data, *in-situ*
1060 measurements and a general circulation model, J. Mar. Syst., 65, 484–508,
1061 doi:10.1016/j.jmarsys.2005.02.006.

1062 Roblou, L., Lamouroux, J., Bouffard, J., Le Henaff, M., Lombard, A., Marsaleix, P., De Mey,
1063 P., 2010. Post-processing altimeter data toward coastal applications and integration into
1064 coastal models. Book Chapter of “Coastal Altimetry” (Book), Springer Verlag Edition,
1065 Editors: Stefano Vignudelli, Andrey Kostianoy, Paolo Cipollini and Jêrôme Benveniste.

1066 Rubio, A., Barnier, B., Jordà, G., Espino, M., Marsaleix, P., 2009. Origin and dynamics of
1067 mesoscale eddies in the Catalan Sea (NW Mediterranean): Insight from a numerical
1068 model study, J. Geophys. Res., 114, C06009, doi:10.1029/2007JC004245.

Ruiz, S., L. Renault, B. Garau, and J. Tintoré (2012), Underwater glider observations and modeling of an abrupt mixing event in the upper ocean, Geophys. Res. Lett., 39, L01603, doi:10.1029/2011GL050078.

Ruiz, S., Pascual, A., f, B., Faugere, Y., Alvarez, A., Tintoré J., 2009b. Mesoscale dynamics of the Balearic Front, integrating glider, ship and satellite data. Journal of Marine Systems, 78, S3-S16, doi: 10.1016/j.jmarsys.2009.01.007.

Ruiz, S., Pascual, A., Garau, B., Pujol, I. and Tintore, J., 2009a. Vertical motion in the upper ocean from glider and altimetry data. Geophysical Research Letters, 36: L14607, doi:10.1029/2009GL038569.

Sackmann, B. S., M. J. Perry, AND C. C. Ericksen. 2008. Seaglider observations of variability in daytime fluorescence quenching of chlorophyll-a in Northeastern Pacific coastal waters. Biogiosciences Discuss. 5: 2839–2865.

Send, U., Font, J., Krahmann, G., Millot, C., Rhein, M., Tintore, J., 1999. Recent advances in observing the physical oceanography of the western Mediterranean Sea, Prog. Oceanogr.,5 44, 37–64, 1999. 587, 591.

Shchepetkin, A. F. and McWilliams, J.C., 2005. The regional oceanic modeling system (ROMS) : a split-explicit, free-surface, topography-following-coordinate oceanic model. Ocean Modelling,9:347–404.

Skamarock, W.C., Klemp, J.B., Dudhia, J., O. Gill, D., Barker, D.M., Duda, M.G., Huang, X.-Y., Wang, W., Powers, J.G., 2008. A description of the Advanced Research WRF Version 3, NCAR/TN–475+STR NCAR TECHNICAL NOTE, June 2008. http://www.mmm.ucar.edu/wrf/users/docs/arw_v3.pdf

Smith, W. H. F., and Sandwell, D.T., 1997. Global sea floor topography from satellite altimetry and ship depth soundings. Science 277:1956–1962.

SSALTO/DUACS User Handbook: (M)SLA and (M)ADT Near-Real Time and Delayed Time Products. SALP-MU-P-EA-21065-CLS

Testor, P. and 44 co-authors,2010. Gliders as a component of future observing systems, in Proceedings of the "OceanObs'09: Sustained Ocean Observations and Information for Society" Conference (Vol. 2), Venice, Italy, 21-25 September 2009, Hall, J., Harrison D.E. and Stammer, D., Eds., ESA Publication WPP-306.

Tintoré, J., G. Vizoso, B. Casas, L. Renault, S. Ruiz, B. Garau, A. Pascual, M. Martínez-Ledesma, LL. Gomez-Pujol, A. Orfila (2012), SOCIB: the impact of new marine infrastructures in understanding and forecasting the coastal oceans: some examples from the Balearic Islands in the Mediterranean Sea. Planning repeated basin-wide surveys for climatic studies in the Mediterranean Sea. Supetar (Island of Brac, Croatia), 11 - 14 May 2011. CIESM Workshops Monographs (in press.)

Tintoré, J., Wang, D. P., La Violette, P. E. 1990. Eddies and thermohaline intrusions of the shelf/slope front off Northeast Spain. J. Geophys. Res., 95, 1627-1633.

Vignudelli S., Kostianoy A.G., Cipollini P., Benveniste J. (eds.), *Coastal Altimetry*, Springer-Verlag Berlin Heidelberg, 578 pp, 2011. DOI: 10.1007/978-3-642-12796-0

Vignudelli, S., P. Cipollini, L. Roblou, F. Lyard, G. P. Gasparini, G. Manzella, and M. Astraldi (2005), Improved satellite altimetry in coastal systems: Case study of the Corsica Channel (Mediterranean Sea), Geophys. Res. Lett., 32, L07608, doi:10.1029/2005GL022602

Volkov, D. L., Lee, T., Fu, L.-L., 2008. Eddy-induced meridional heat transport in the ocean, Geophys. Res. Lett., 35, L20601, doi:10.1029/2008GL035490.

Wang F., Vieira M., Salat J., Tintoré J. & La Violette P.E, 1988. A shelf/slope filament off the Northeast Spanish Coast. *J. Mar. Res.*, 46, 321-332.

Tables:

Products/ satellite	Resolution / Spatial filtering	Mean Sea Surface / MDT	Quality control procedure	Time sampling / cycles
PISTACH / JASON-2 (track 70) (Coastal and Hydrology Altimetry product handbook, 2010)	20hz ~ 350 m 1hz ~ 7km / 15 km	MSS Cls01 (http://www.aviso.oceanobs.com) / MDT (Rio et al , 2007)	As in Bouffard et al (2010)	10 days / cycle 4 and cycle 5
Gridded / Multi-missions (SSALTO/DUACS User Handbook)	1/8 degree / 42 km	MSS Cls01 (http://www.aviso.oceanobs.com) / MDT (Rio et al , 2007)	Standard	7 days / time-averaged

Table 1 - Main altimetric data characteristics

		Mean	Altimetry Correlation	Glider Correlation
Altimetry	Cycle 4	7.9	1	0.91
	Cycle 5	6.8	1	0.73
Glider	Northward	5.6	0.91	1
	Southward	15.0	0.73	1

Table 2 - Statistical comparisons between across-track absolute surface geostrophic current (mean in cm/s) from along-track altimetry (PISTACH) and glider observations

Absolute surface geostrophic current	Temperature (from glider)		Salinity (from glider)	
	0 m -50 m	-50 m -180 m	0 m -50 m	-50 m -180 m
Glider	0.05	-0.06	0.17	0.81
Altimetry	-0.04	-0.13	0.11	0.67

Table 3 - Mean spatial correlations (function of depth) between across-track surface absolute geostrophic currents (from glider northward transect and altimetry cycle 4) and temperature and salinity gradient from glider measurements

Area		Mean	STD	Absolute difference
SST	Model	26.0	0.8	0.5
	Satellite	26.0	1.0	
EKE	Model	170	35	52
	satellite	221	20	
EKE from SLA	Model	58	16	18
	Satellite	41	18	

Table 4 - Statistical comparisons between model and AVHRR SST (in °C), EKE and EKE derived from the SLA (in cm^2/s^2)

Correlation with surface absolute geostrophic current (from Model)	Temperature (from model)		Salinity (from model)	
	0 m -50 m	-50 m -180 m	0 m -50 m	-50 m-180 m
	0.35	-0.30	0.64	0.53

Table 5 - Mean spatial correlations (function of depth) between across-track surface absolute geostrophic currents and temperature and salinity gradient (from model)

		Mean	Correlation with glider
Glider	Northward	2.2	1
	Southward	2.7	1
Model	Northward	1.6	0,91
	Southward	1.3	0.52

Table 6 Statistical comparisons between across-track relative surface geostrophic current (/180m) from model and glider observations (mean is in cm/s)

Area		Mean	STD	Absolute difference
ZONE 1	Model	26.1	0.8	0.4
	satellite	26.3	1.1	
ZONE 2	Model	26.0	0.8	0.4
	Satellite	25.9	1.0	
ZONE 3	Model	25.8	0.8	0.3
	satellite	25.9	1.0	
ZONE 4	Model	26.0	0.8	0.4
	Satellite	26.0	1.0	

Table A1 - Statistical comparisons between model and AVHRR SST (in °C, ref to Figure 5 for the Zone locations)

Area		Mean	STD	Absolute difference
ZONE 1	Model	170	20	21
	satellite	169	30	
ZONE 2	Model	230	65	53
	Satellite	270	44	
ZONE 3	Model	105	52	135
	satellite	240	25	
ZONE 3 (from SLA)	Model	53	27	18
	satellite	41	20	
ZONE 4	Model	182	41	40
	Satellite	178	40	

Table A2 - Statistical comparisons between model and AVISO EKE (in cm^2/s^2, ref to Figure 5 for the Zone locations)

Figure-1
Click here to download high resolution image

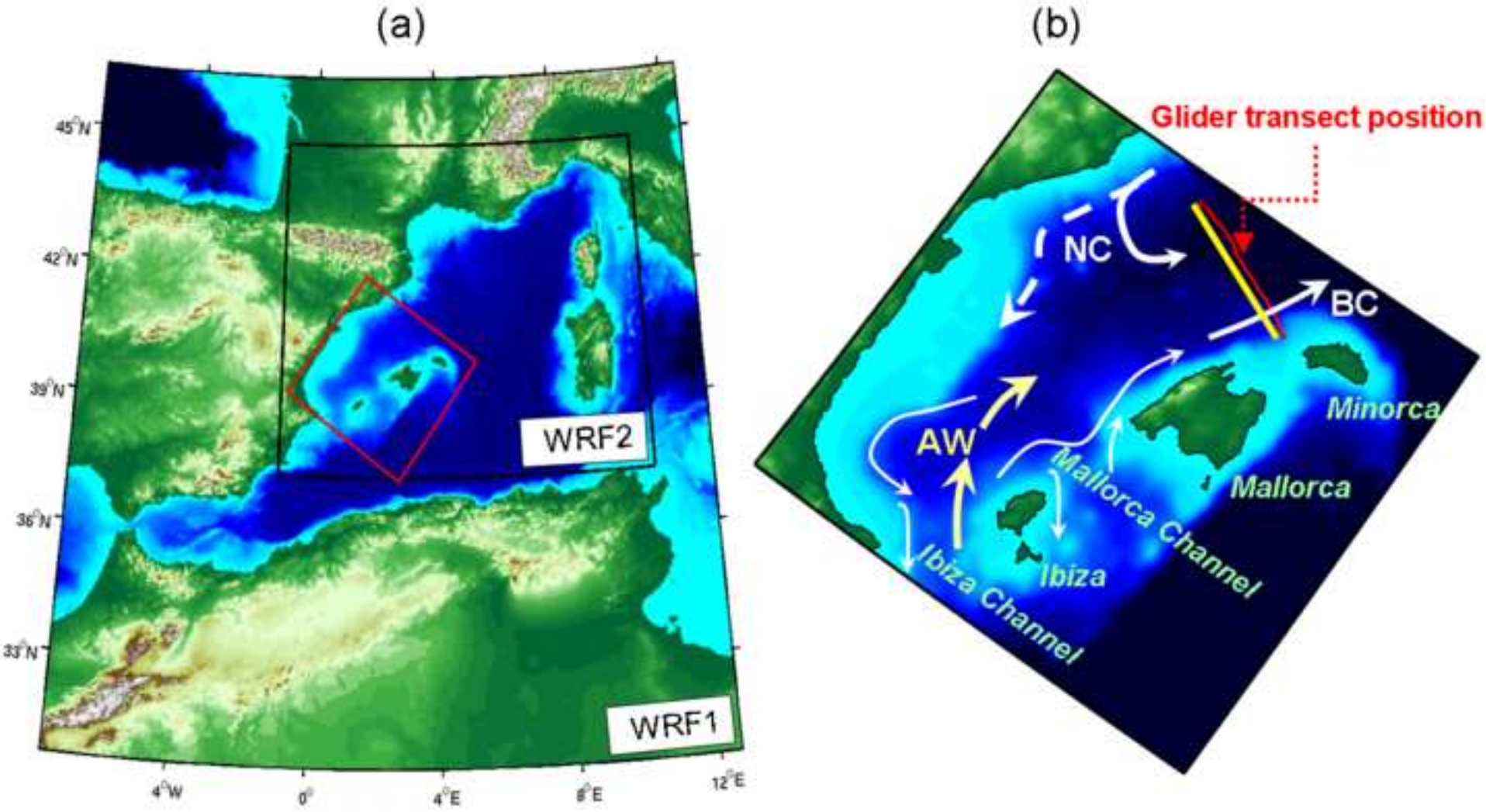

Figure-2
Click here to download high resolution image

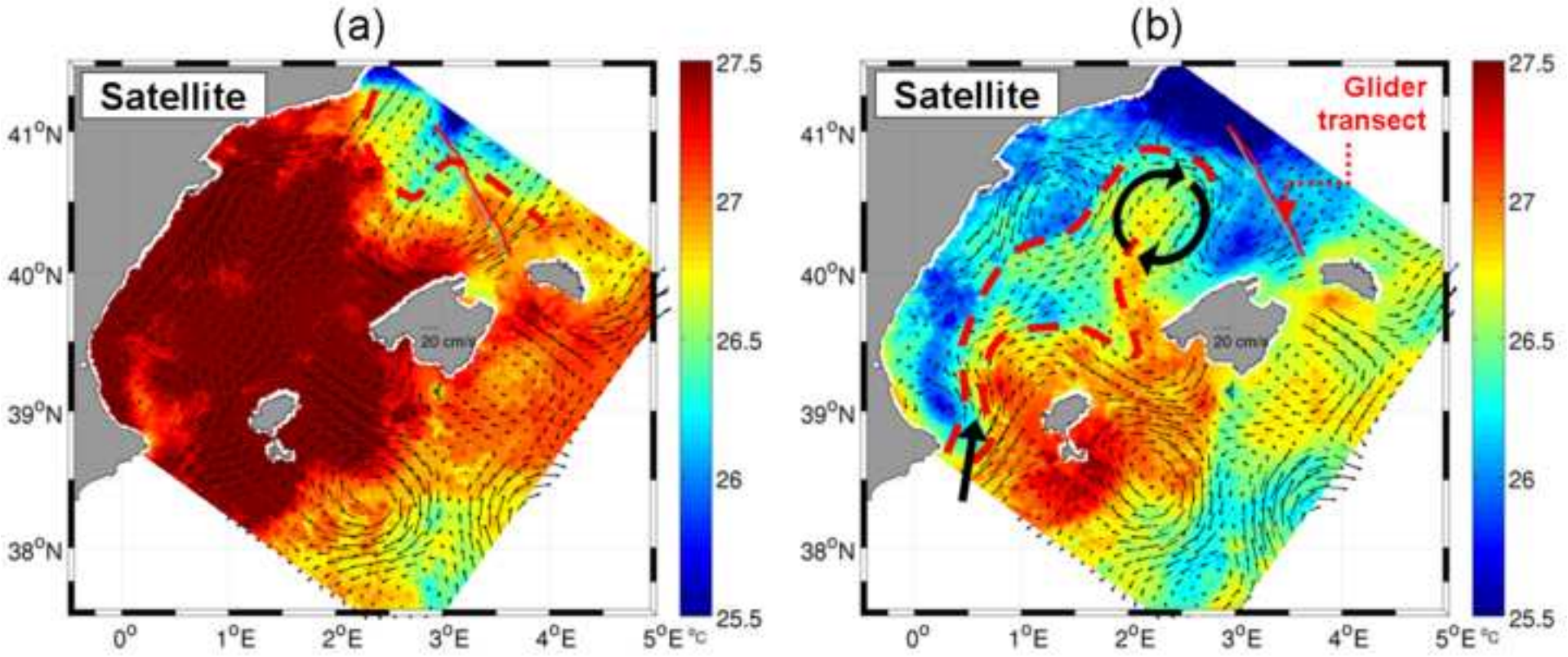

Figure-3

Click here to download high resolution image

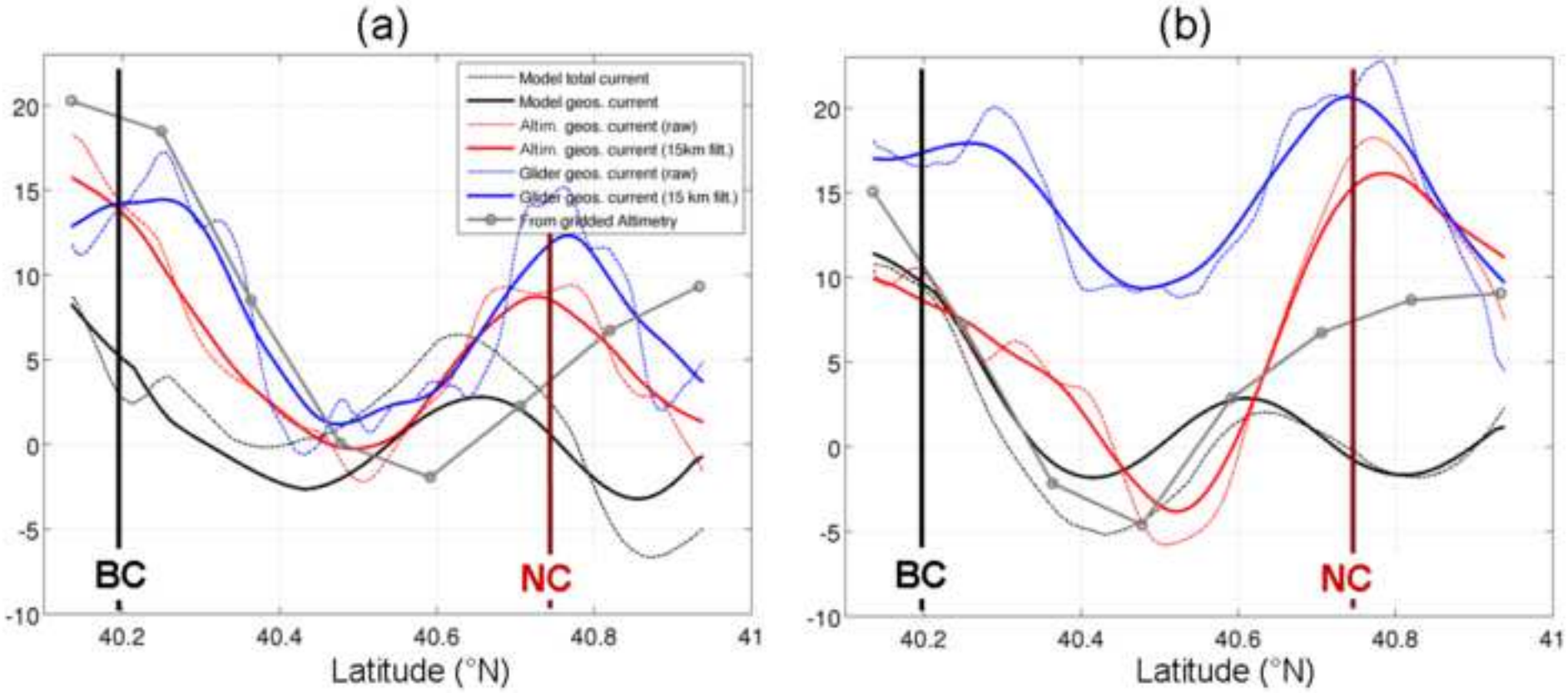

Figure-4

Click here to download high resolution image

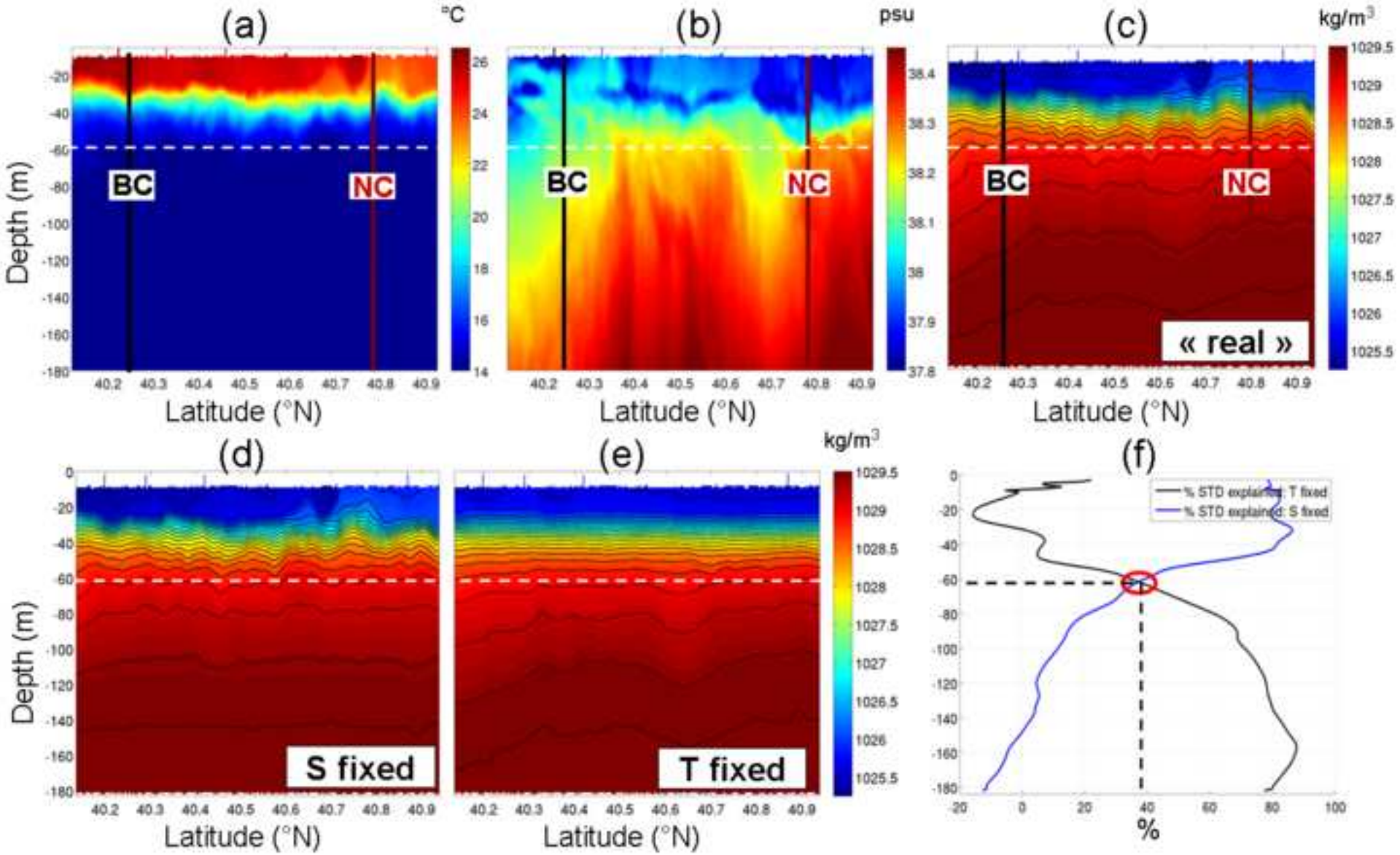

Figure-5

Click here to download high resolution image

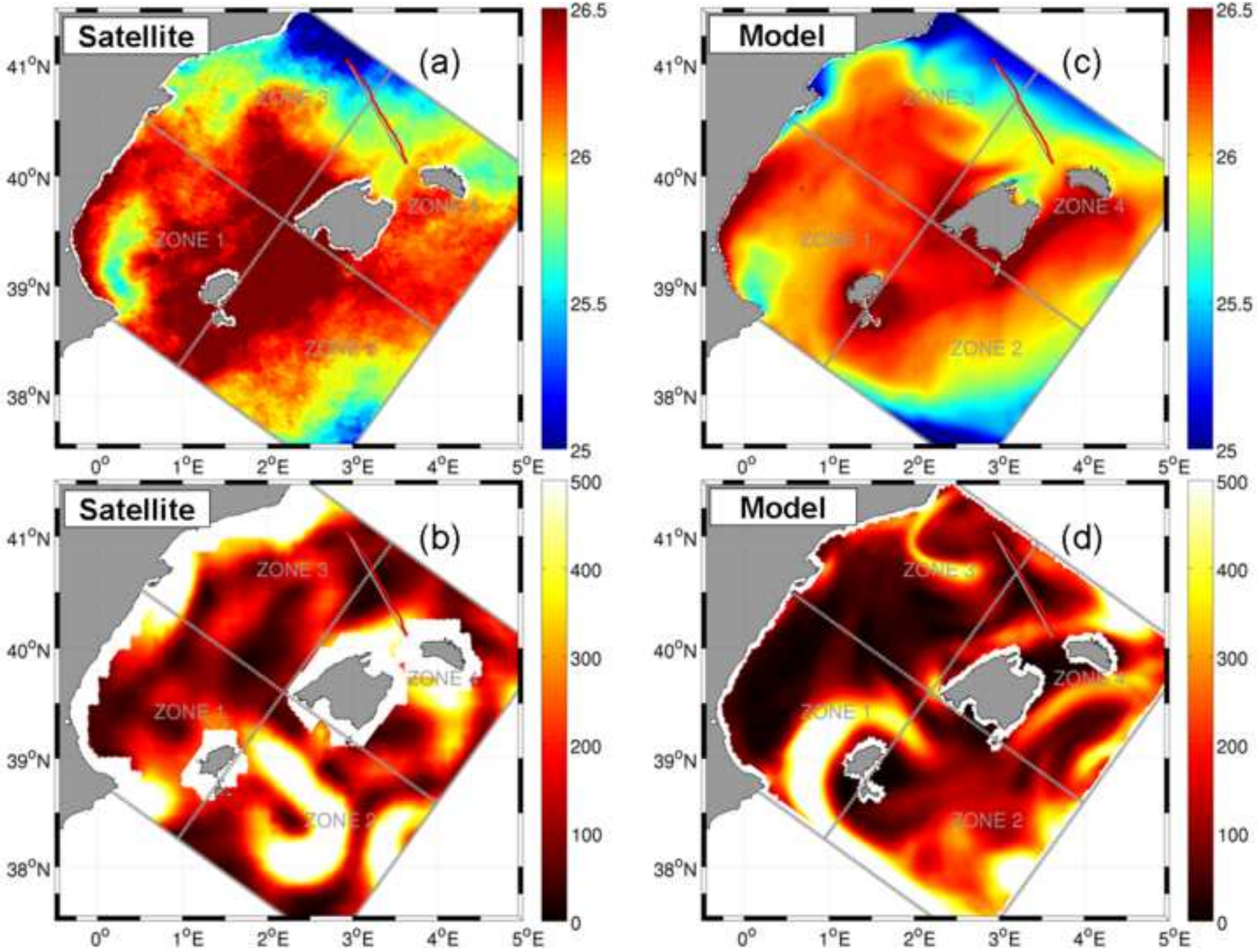

Figure-6

Click here to download high resolution image

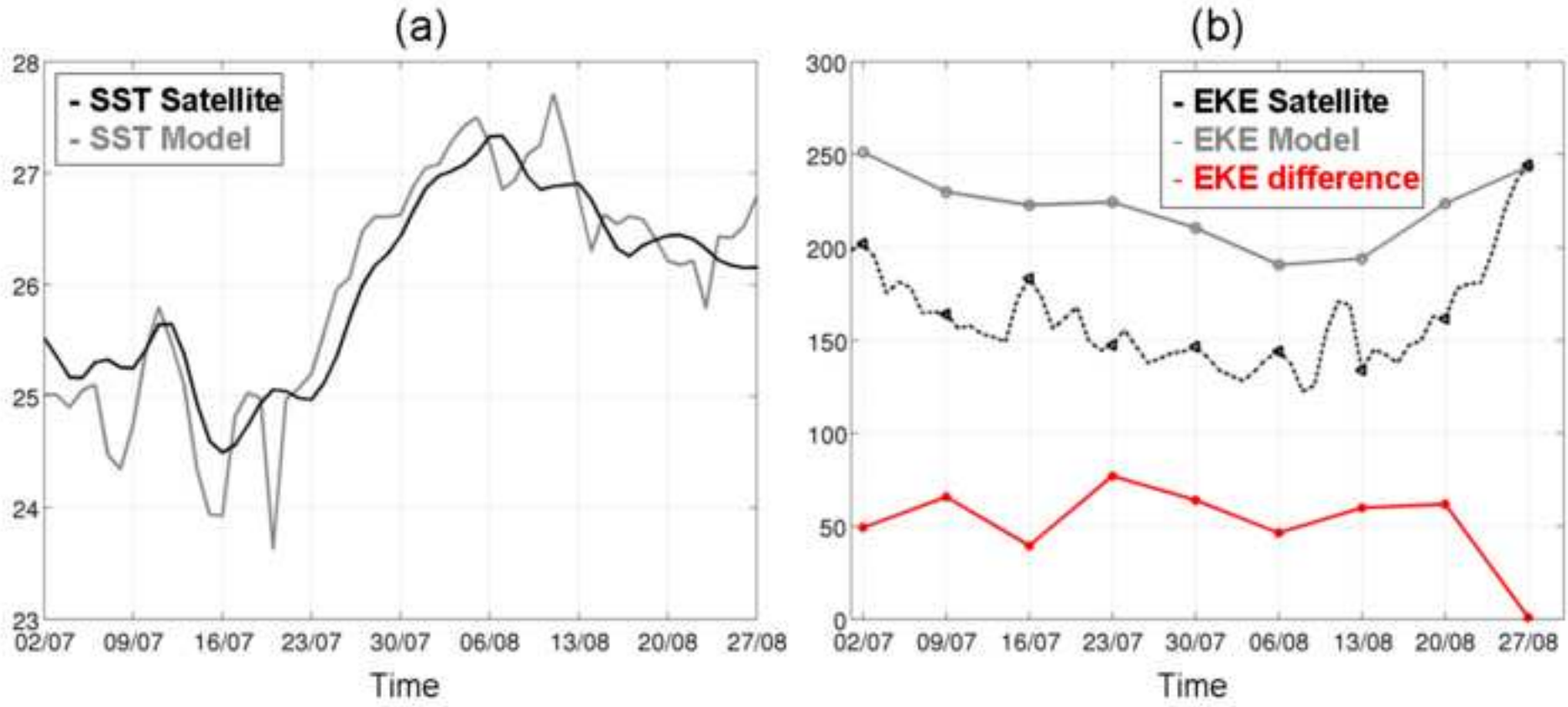

Figure-7

Click here to download high resolution image

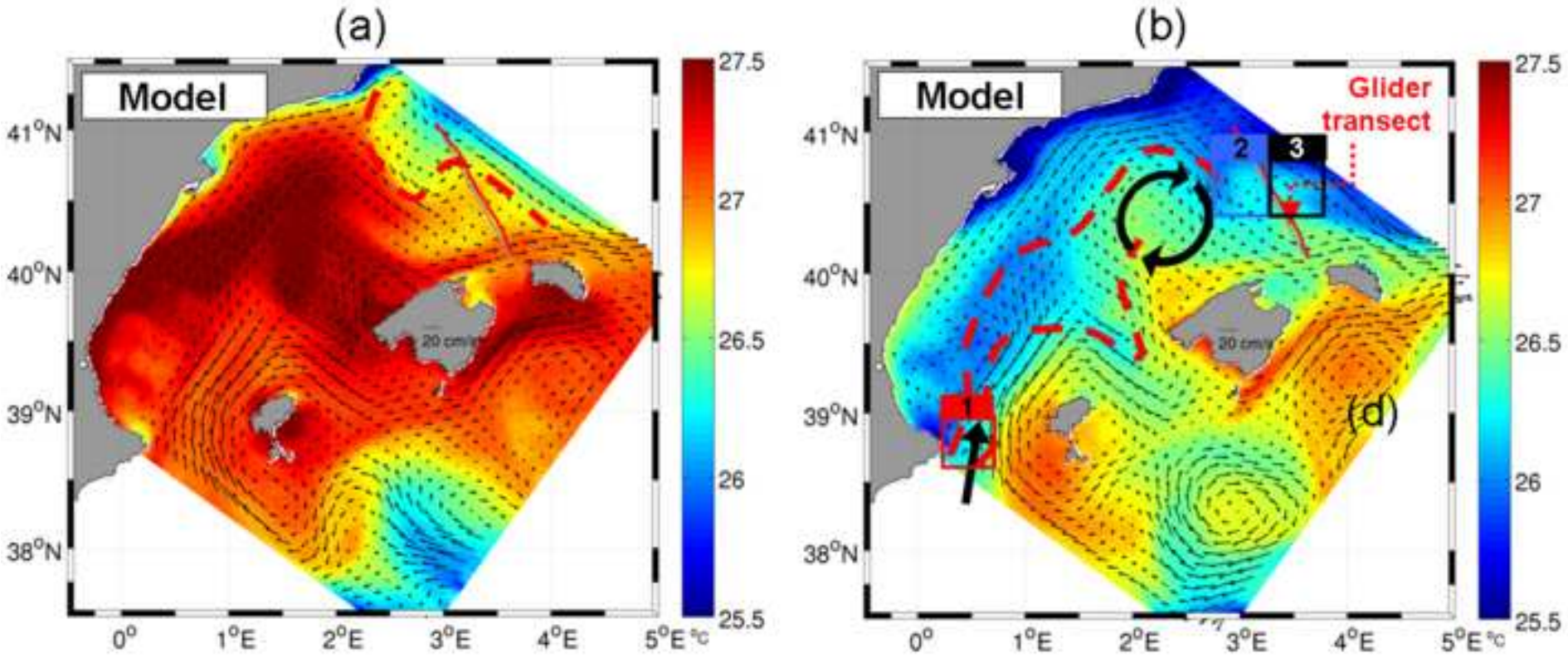

Figure-8

Click here to download high resolution image

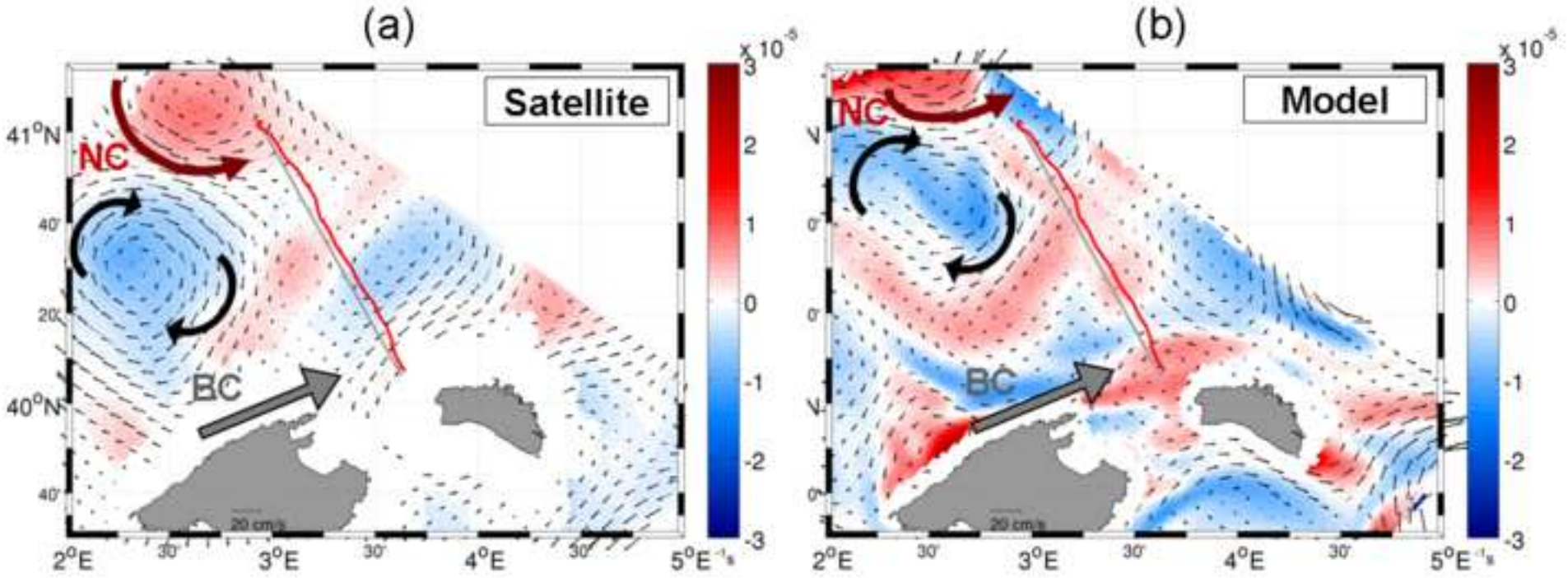

Figure-9

Click here to download high resolution image

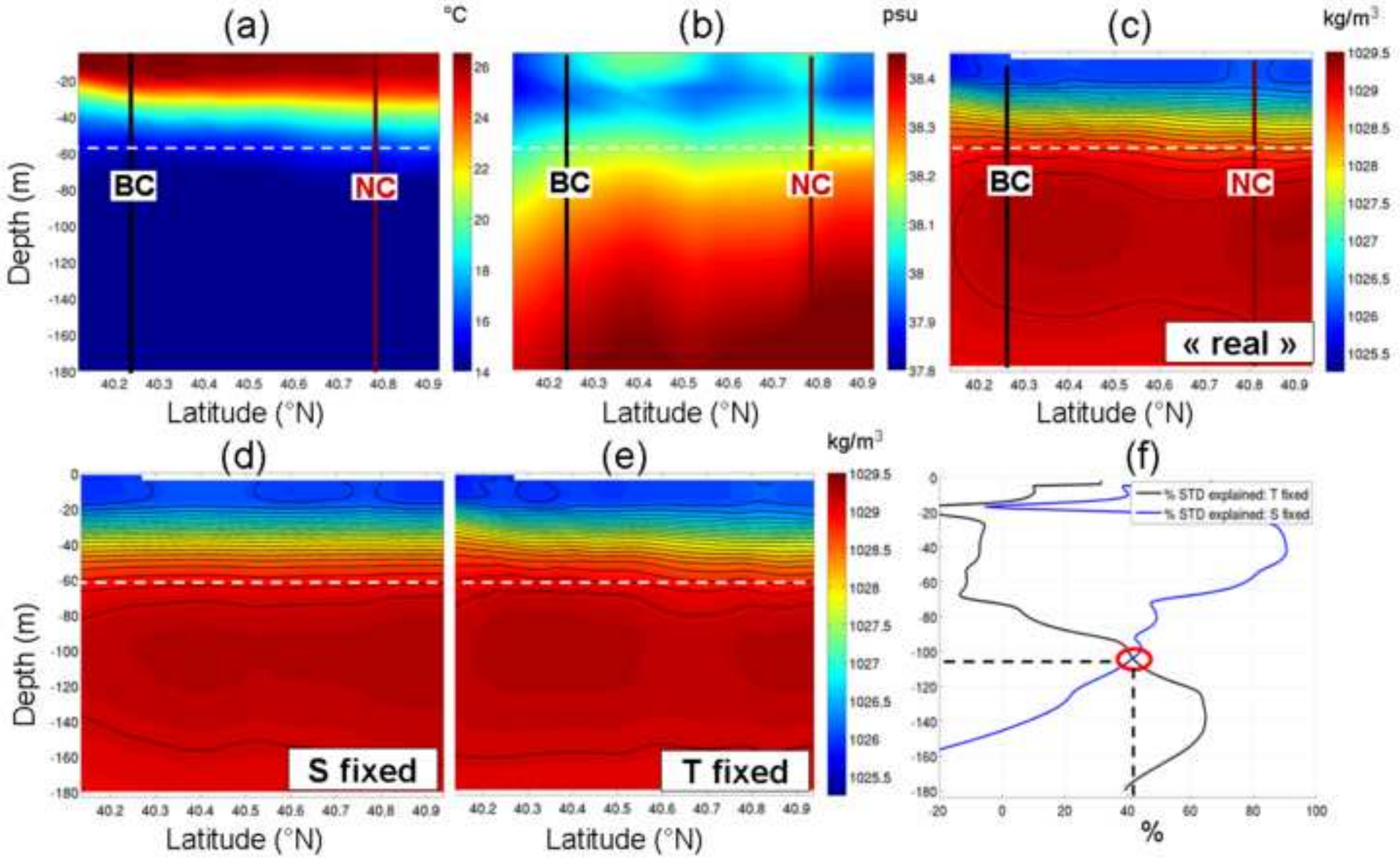

Figure-10

Click here to download high resolution image

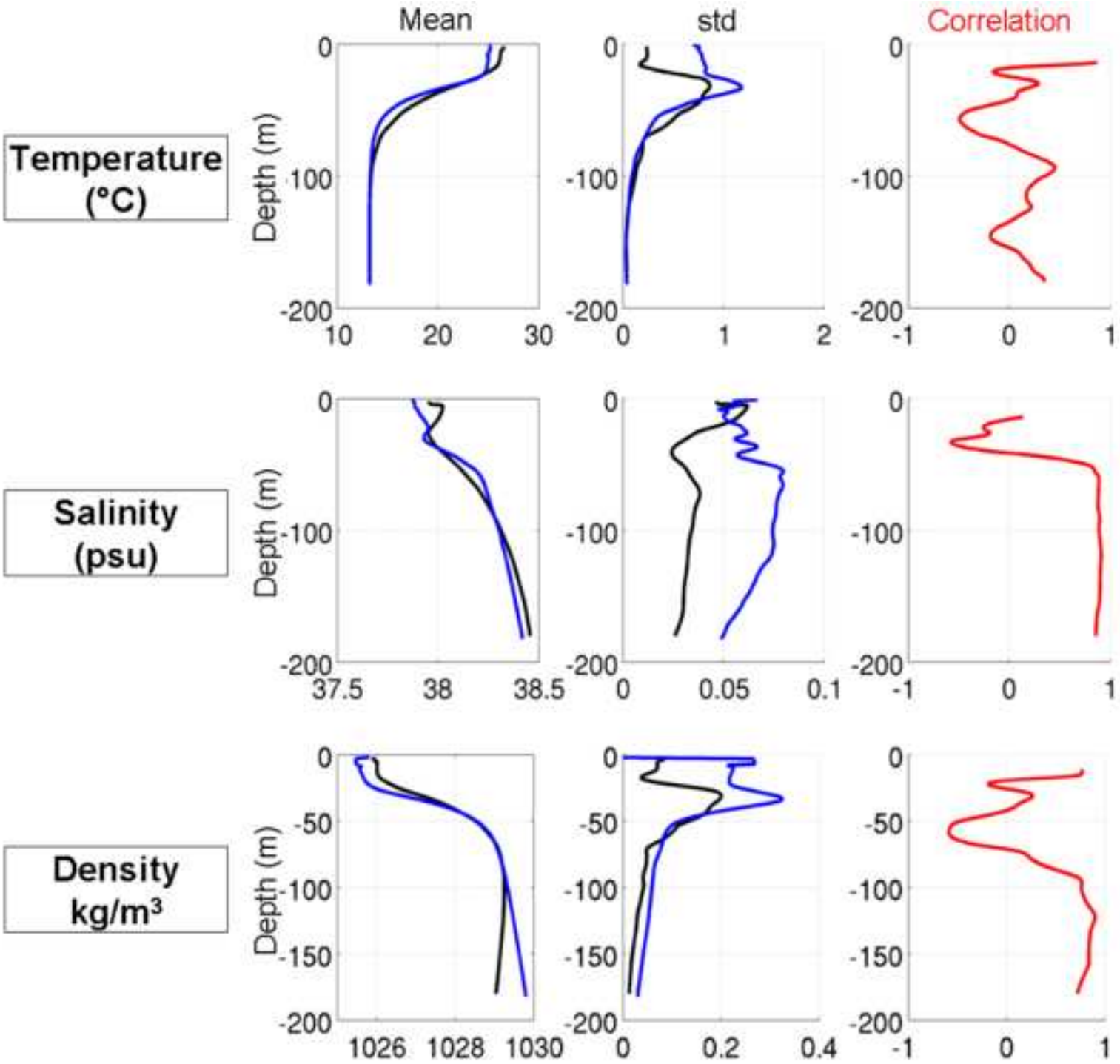

Figure-11

Click here to download high resolution image

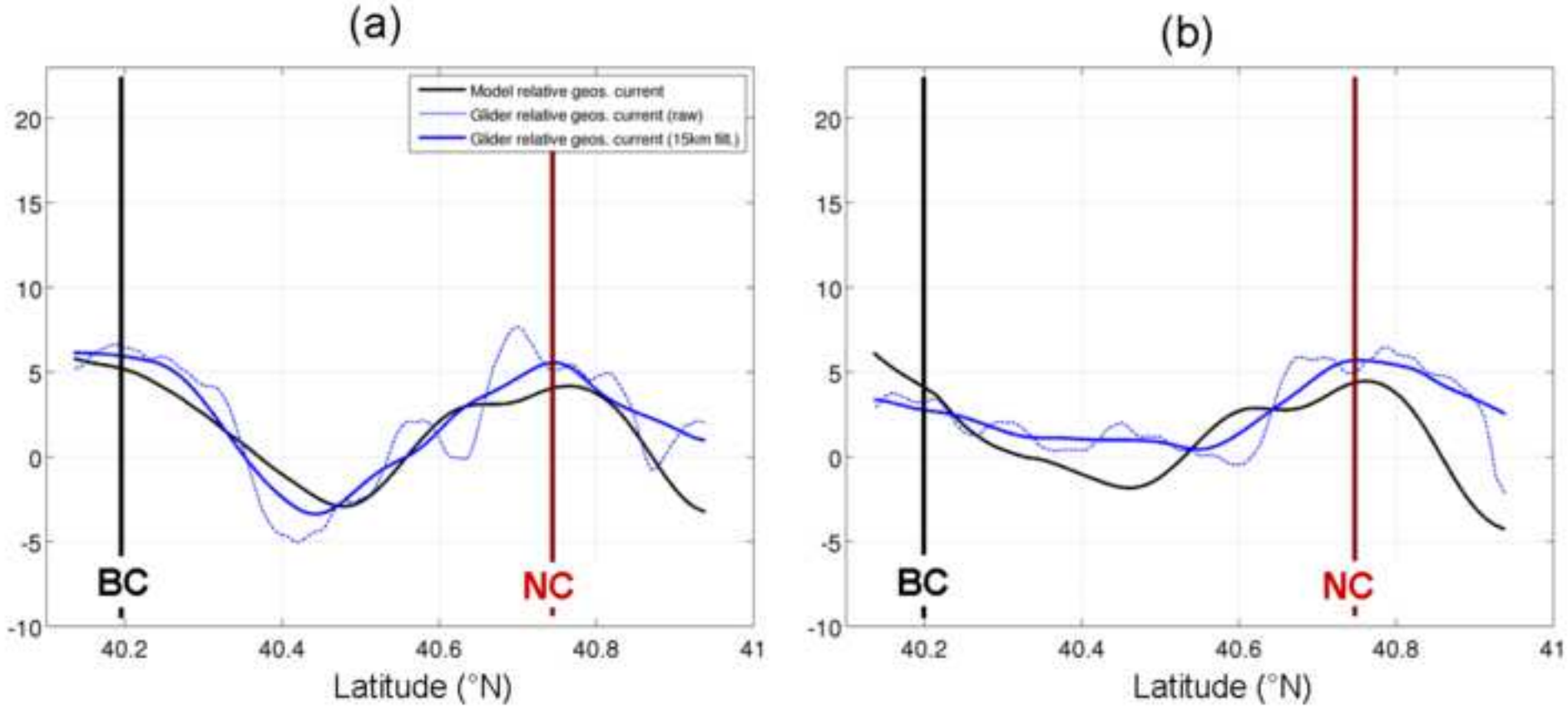

Figure-12
Click here to download high resolution image

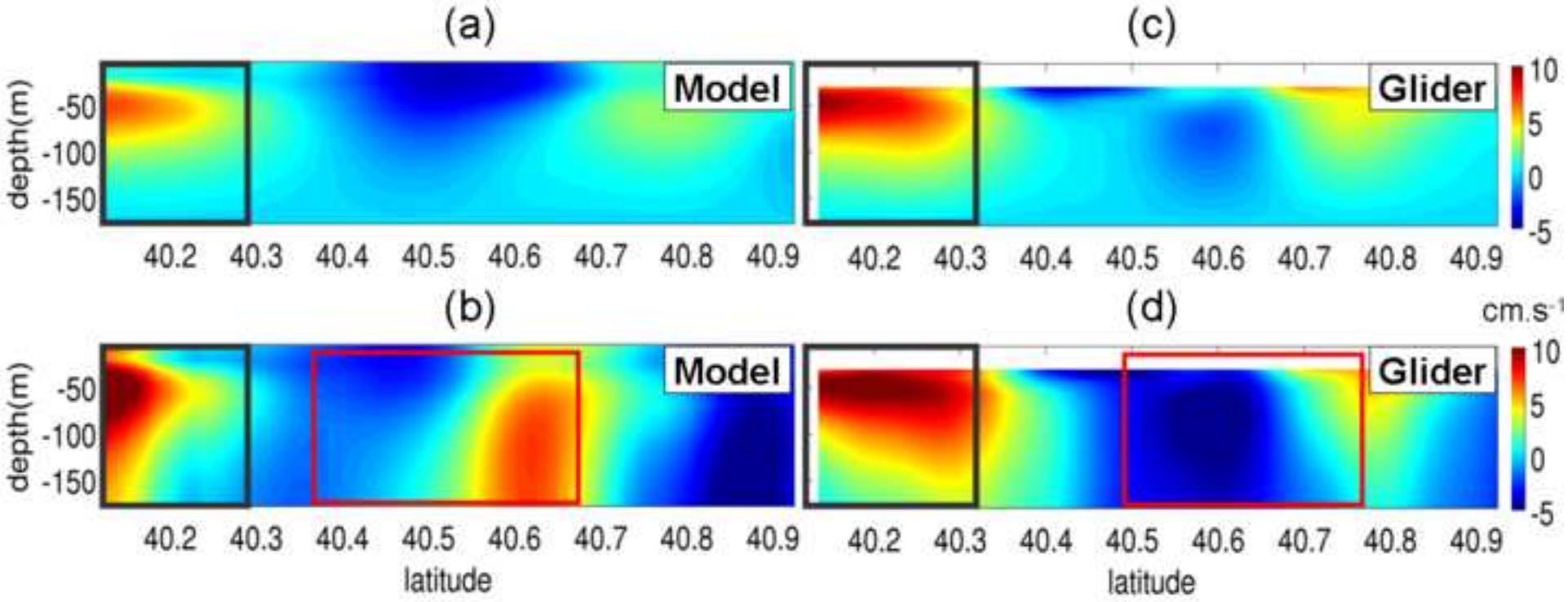

Figure-13

Click here to download high resolution image

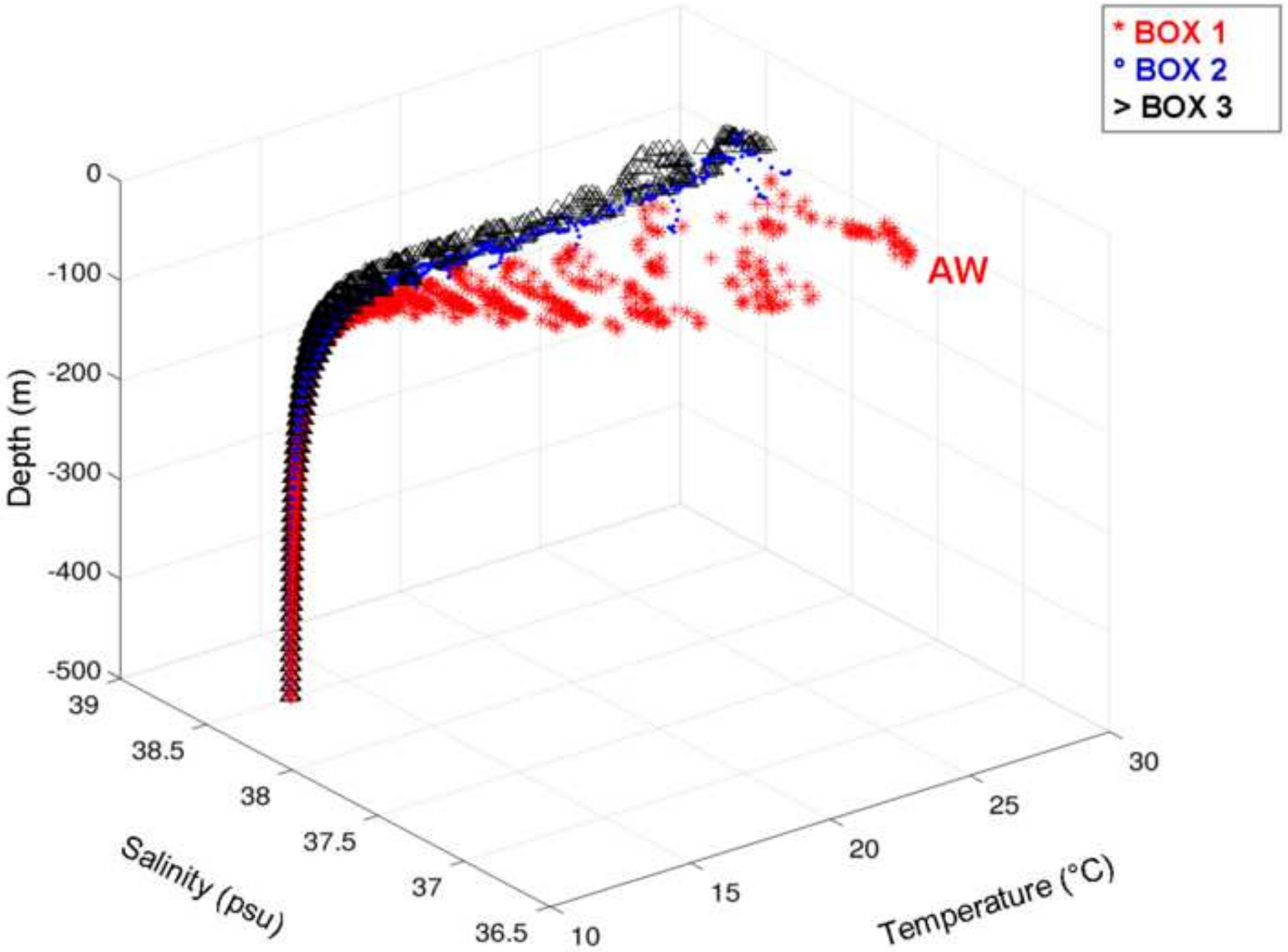

Figure-14

Click here to download high resolution image

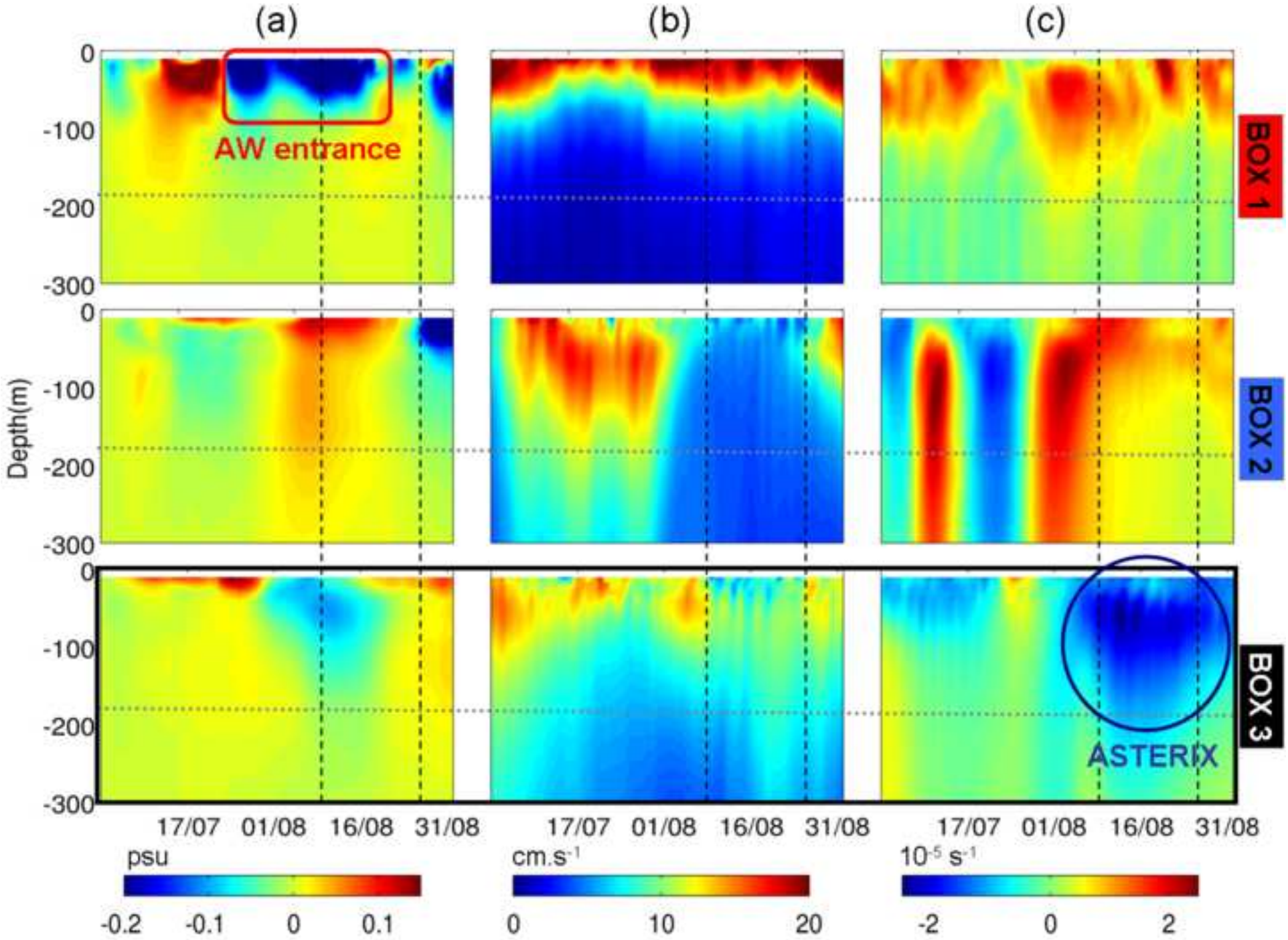

Figure-15

Click here to download high resolution image

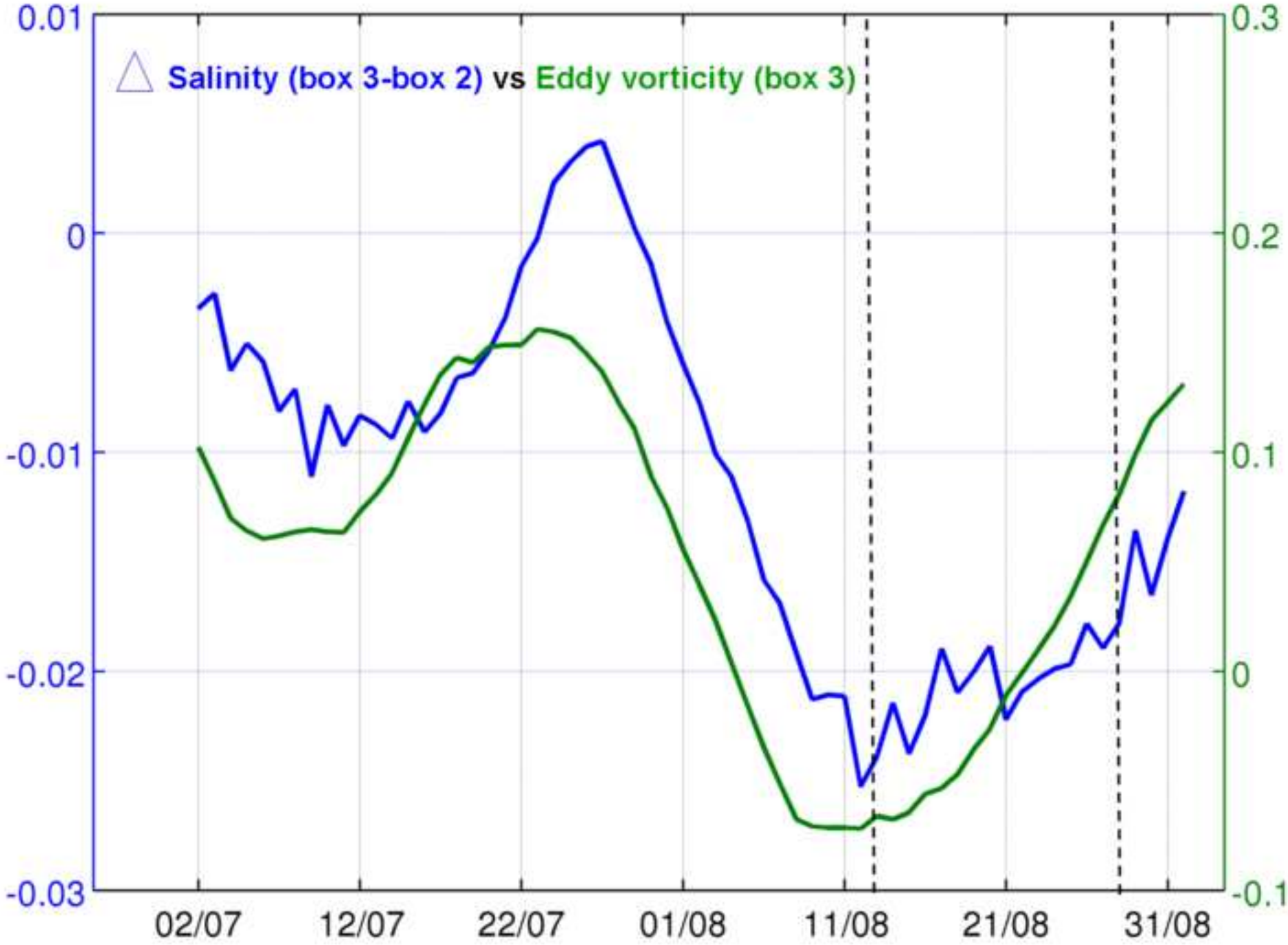

Figure-16

Click here to download high resolution image

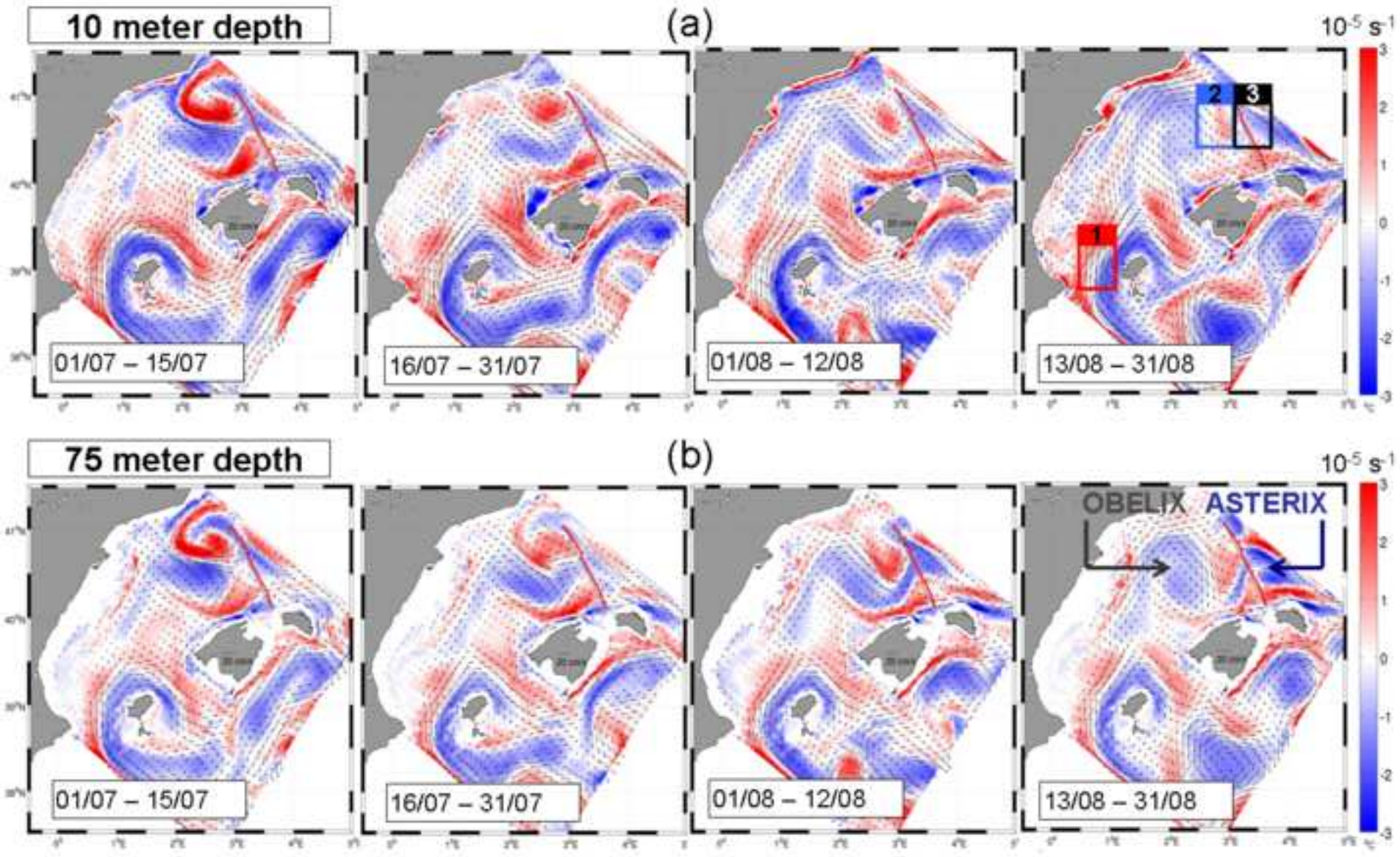

Figure-A1 (related to Appendix A)
Click here to download high resolution image

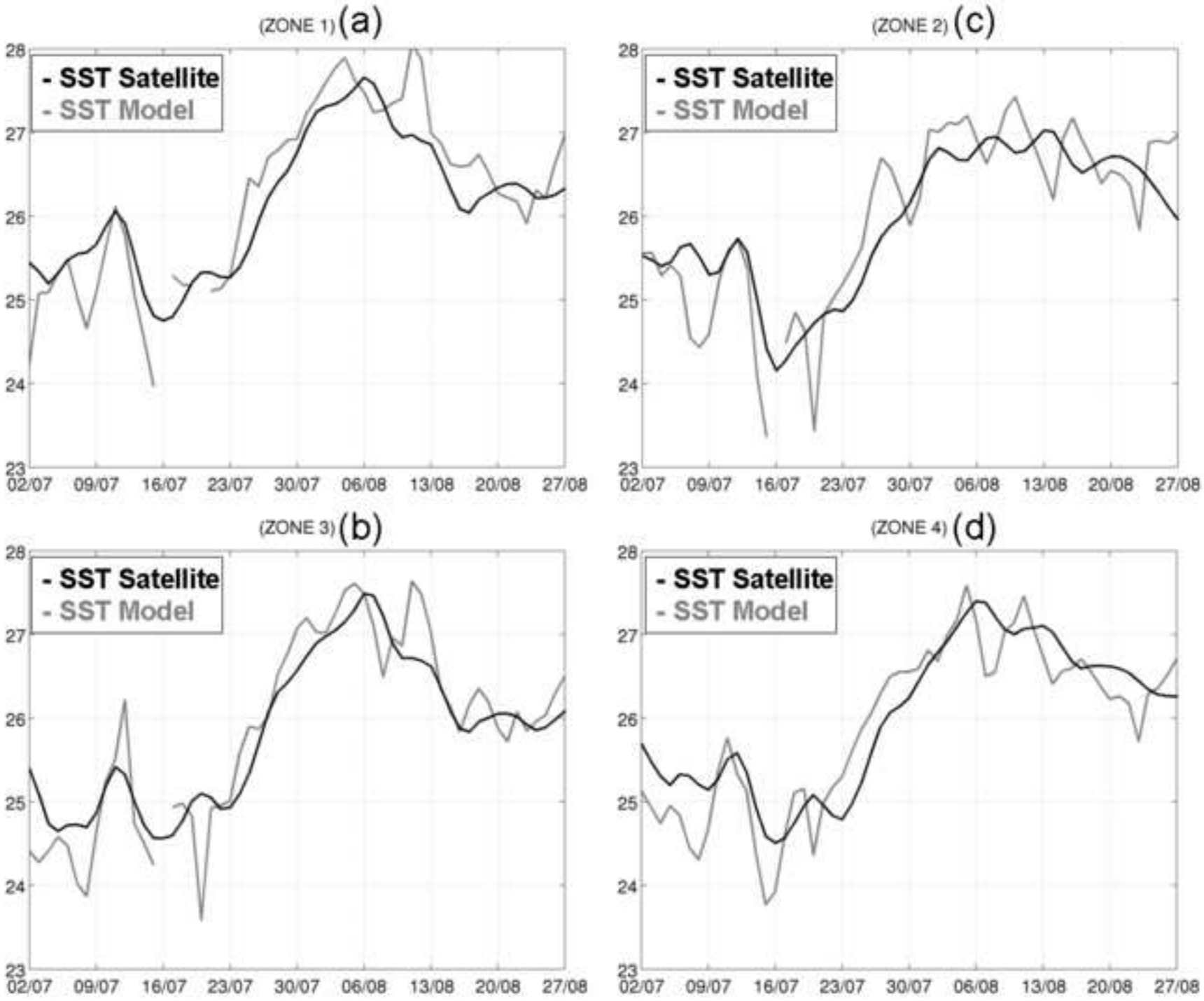

Figure-A2 (related to Appendix A)
Click here to download high resolution image